PRODUCTION FORECASTING FOR SHALE OIL: WORKFLOW

A Thesis

Presented to

the Faculty of the Department of Chemical and Biomolecular Engineering

University of Houston

In Partial Fulfillment

of the Requirements for the Degree

Master of Science

in Petroleum Engineering

by

Mazaruny Rincones

December 2014

PRODUCTION FORECASTING FOR SHALE OIL: WORKFLOW

_____

Mazaruny Rincones

Approved:

_____

Chair of the Committee
Dr. W. John Lee,
Hugh Roy and Lillie Cranz Cullen
Distinguished University Chair
Professor
Petroleum Engineering

Committee Members:

_____

Dr. Arthur B. Weglein
Hugh Roy and Lillie Cranz Cullen
Distinguished University Chair in
Physics
Director, Mission-Oriented Seismic
Research Program (M-OSRP)
Professor, Dept. of Physics
Professor, Dept. of Earth and
Atmospheric Sciences

_____

Dr. Konstantinos Kostarelos
Associate Professor
Petroleum Engineering

_____

Dr. Suresh Khator,
Associate Dean
Cullen College of Engineering

_____

Dr. Michael Harold,
Department Chair
Chemical and Biomolecular
Engineering

ACKNOWLEDGEMENTS

Thanks to God for giving me the gift of life and health.

I cannot thank Dr. John Lee enough for his invaluable contributions to not only my thesis work but my life; he will be a lifelong mentor and friend.

Thanks to Dr. Weglein and Dr. Kostaleros for taking time to be on my committee. It is an honor for me to be part of their careers.

Special mention to Dr. Jeff Rutledge from Marathon Oil, without whose help none of this work would have been possible, and to Karen Olson, my unconditional industry mentor and friend.

Special Thanks to Mr. Chen of Kappa and Schlumberger for providing the software to make this research possible.

Thanks to Ms. Anne Sturm for her continuous support through this entire experience.

Without my family and friends this journey would simply not exist; thanks to Py for being my partner in life. Special thanks to my friends Diego Molinari, Ayush Rastogi, Matteo Marongiu Porcu and Jenny Graterol for their contribution to this research.

PRODUCTION FORECASTING FOR SHALE OIL: WORKFLOW

An Abstract

of a

Thesis

Presented to

the Faculty of the Department of Chemical and Biomolecular Engineering

University of Houston

In Partial Fulfillment
of the Requirements for the Degree
Master of Science
in Petroleum Engineering
by

Mazaruny Rincones

December 2014

ABSTRACT

With the demand for oil rising, unconventional oil reservoirs have taken a prominent role in the United States as a source of crude oil. Different methodologies to estimate reserves for shale gas and coal bed methane have, thus far, proved to be reliable, but no simple yet accurate workflow has been generally accepted to forecast production and estimate reserves for shale oil. To fill this gap in technology, we proposed and validated a workflow that integrates analytical methods with empirical methods. The final methodology is both easily applied and accurate. In developing the final workflow, we evaluated several alternatives, most of which proved to be unsuitable. We also investigated the use of a filter to eliminate outliers in a systematic way, as proposed by Rastogi (2014).

The workflow was successfully applied to three of four volatile oil wells in the Eagle Ford shale, with similar results. The analytical model that best matched the wells is called the Stimulated Reservoir Volume (SRV) Bounded Model by the software marketer Kappa. We tested this and other models using a Beta test version of new Kappa software. While accurate, this modeling approach is too time consuming for routine use. We found that a simple empirical approach that led to the same results as the analytical model was a 3-segment Arps decline model. The early flow regime was transient linear for all the wells; thus an Arps "*b*" parameter of two was appropriate. When boundary-influenced flow (BIF) appeared later, *b*-values of 0.2 were found appropriate. The initial decline rate (D_i) value during BIF was modified in mid-segment leading to a distinct third segment. Our workflow also led to reliable forecasts of production (to date) of the gas-oil ratio for the three wells.

TABLE OF CONTENTS

LIST OF FIGURES

LIST OF TABLES

NOMENCLATURE

Variables:

a	=	$Model\ Parameter,\ D^{-1}$
A	=	$Drainage\ area,\ \ ft^2$
b	=	$Arps'\ decline\ exponent, dimensionless$
B_{oi}	=	$Oil\ formation\ volume\ factor, rb/st$b
c_f	=	$Formation\ compressibilty, psi^{-1}$
c_{ti}	=	$Total\ initial\ compressibility, psi^{-1}$
D	=	$Reciprocal\ of\ loss\ ratio, D^{-1}$
D_i	=	$Initial\ decline\ constant\ for\ exponential\ and\ hyperbolic\ rate\ relation, D\^(-1)$
F_c	=	$Fracture\ conductivity, md-ft$
Q	=	$Cumulative\ oil\ production, STB$
h	=	$Formation\ thickness, ft$
k	=	$Formation\ permeability, md$
L_w	=	$Horizontal\ well\ length, ft$
n	=	$Time\ exponent\ for\ rate-time\ models, dimensionless$
n_f	=	$Number\ of\ transverse\ hydraulic\ fractures\ intersecting\ the\ horizon\ wellbore$
P	=	$Pressure, psia$
$\bar{p}$	=	$Average\ reservoir\ pressure, psi$
p_i	=	$Initial\ reservoir\ pressure, psia$
p_{cf}	=	$Flowing\ casing\ pressure, psia$
p_{tf}	=	$Flowing\ tubing\ pressure, psia$
q	=	$Production\ rate, stb/d$
q_i	=	$Initial\ production\ rate, stb/d$
r_e	=	$Outer\ boundary\ radius, ft$
r_w	=	$Wellbore\ radius, ft$
s	=	$Skin\ factor, dimensionless$
T	=	$Reservoir\ temperature$, °F
x_f	=	$Fracture\ half\ length, ft$

CHAPTER 1 INTRODUCTION

The unconventionals energy revolution started with shale gas in the Barnett Shale; this approach quickly migrated to shale oil propelled by average oil prices over $100/STB. Advances in hydraulic fracturing and horizontal drilling have been the key enablers for commercial production of hydrocarbons in the majority of shale developments. Despite the apparent success in shale oil exploration and production, there are still many unknowns in production forecasting and reserves estimations.

Petroleum engineering has evolved through the years to recognize the characteristics that will make a conventional reservoir commercial. However, for unconventional reservoirs the impact of these characteristics, like porosity, hydrodynamics, traditional phase behavior, permeability and hydrocarbon sourcing are still under study.

Today shale oil is in a period of uncertainty, from drilling and completions techniques, optimal well spacing and, most relevant to this project, reserves estimations and production forecasting in shale oil. Shale oil production has been increasing steadily since 2012 as seen in Figure 1. There was not a wealth of data before that time. Now that five years of production data are available, it can be expected that research on shale oil forecasting will continue to flourish.

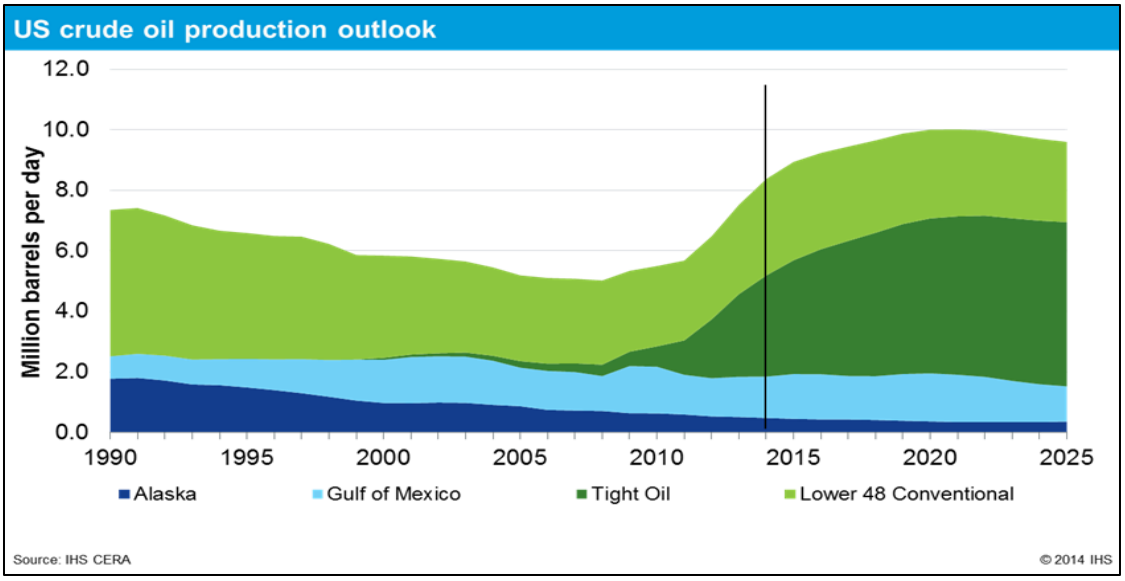

Figure 1 US crude oil production outlook. (Source: IHS CERA.) Notice how the tight oil is the category that is expected to increase the most.

The purpose of this research is to develop a workflow that will help to streamline production forecasting for shale oil reservoirs. This workflow will combine empirical and analytical methods to generate a quick, simple and yet technically sound approach.

The implications of this work are very broad, ranging from the use of current technology and sound theory to evaluate production trends, to quickly preparing data for audits and current legal bodies such as the Securities & Exchange Commission (SEC), and to the time savings that will be critically important when time is an issue and the number of wells to be processed would require more time than is available.

CHAPTER 2 THE WORKFLOW

Our proposed workflow was taken from Clarkson (2013) and applied to the Eagle Ford shale oil. Clarkson's workflow was developed for coal bed methane and dry gas and had previously been applied largely to simulated data. In our proposed workflow, data provided by an operator in the Eagle Ford was used.

The data set included four wells with production history and one representative PVT (Pressure-Volume-Temperature fluid behavior) data set for the entire oil reservoir. The workflow can be separated into nine major steps, each of which will be explained, and their application and results shown for each well individually.

Well Data:

Well	Effective Horizontal Length (ft)	# stages	Average TVD/tubing depth (ft)	Production method	Reservoir temperature (°F)	Initial pressure (psi)
1	3569	12	11665'	Rod Pump	314	9500
2	3983	14	11600'	Rod Pump	312	9000
3	3897	14	11475'	Rod Pump	310	9000
4	6500	19	11190'	Rod Pump	305	9500

Well completions (all wells):

	Outside diameter (inches)	Inside diameter (inches)
Casing	5.5	4.670
Tubing	2.875	2.441

Oil PVT Data:

Temperature	280	°F
Pressure	9429.7	psia
Saturation pressure (P_b)	3987.7	psia
Solution Gas/Oil Ratio (R_s)	1405	scf/stb
Formation Volume Factor (B_o)	1.9633	B/STB
Average Single –Phase Compressibility (c_o)	1.24088E-5	psi-1
Reservoir Fluid viscosity (μ_o)	0.270822	cp
Reservoir Fluid density (ρ_o)	0.581261	g/cc
Tank Oil Gravity	43.9	^{o}API

Reservoir Data:

Thickness (ft)	150
Porosity (%)	7
Reservoir permeability	millidarcies to nanodarcies
Initial water saturation (%)	30
Initial oil saturation (%)	70
Initial gas saturation (%)	0
Average fracture half length (ft)	250
Wellbore diameter (in.)	2.875
Skin factor	0

STEP 1: ASSESS DATA VIABILITY.

Ilk et al. (2006) and Ilk et al. (2011) drafted an extensive procedure on how to assess production data viability. While these are not the only procedures available, the steps they recommend are easy- to-follow guidelines. This could easily be the most important step in any reservoir analysis; interpretations performed on incomplete or dubious data are not only dangerous but also can generate invalid reservoir/well data and ultimately an incorrect forecast.

In this step the analyst will determine whether there is enough data to proceed with the analysis. All the data should come from direct measurements and not from

uncertain allocations. Daily measurements are preferred since the noise that could be introduced if the rates and pressure are gathered monthly may render the analysis invalid. All liquid data (water and hydrocarbons) should be reported, since water rates are an excellent indicator of fracture fluid clean up.

Preliminary production diagnostics review the well data, rate correlations, production allocation, and identify changes in well architecture. All diagnostics should be completed before any further analysis is performed on the data. Skepticism is recommended when looking at a data set for the first time to avoid applying preconceived ideas that could mask the real nature of the data set.

The four wells data sets available were provided without well histories, PVT data, or bottom hole pressures. The flowing tubing pressures (p_{tf}) and the flowing casing pressures (p_{cf}) were provided with the rate histories. We immediately noticed a sudden change of p_{cf} values to zero. This was not explained on any of the operational notes provided by the operator. Figure 2 to Figure 5 show the values of p_{tf} and p_{cf} vs time.

Further investigation of the data showed that 2 7/8" diameter tubing was commonly installed after a short time of producing through 5.5" P-110 casing. Ignoring these changes would lead to large errors in calculated p_{wf} values and misleading rate appraisals.

We used PIPESIM software to model multiphase flow from the reservoir to the wellhead. This software was used in this step for two different applications: (1) to convert p_{tf} and p_{cf} to p_{wf} by including PVT data and taking into consideration the multiphase flow in the horizontal portion of the well and in the vertical casing or tubing

flow; and (2) to recombine the PVT data provided by the operator to reconcile the observed GOR and the GOR estimated from PVT analysis.

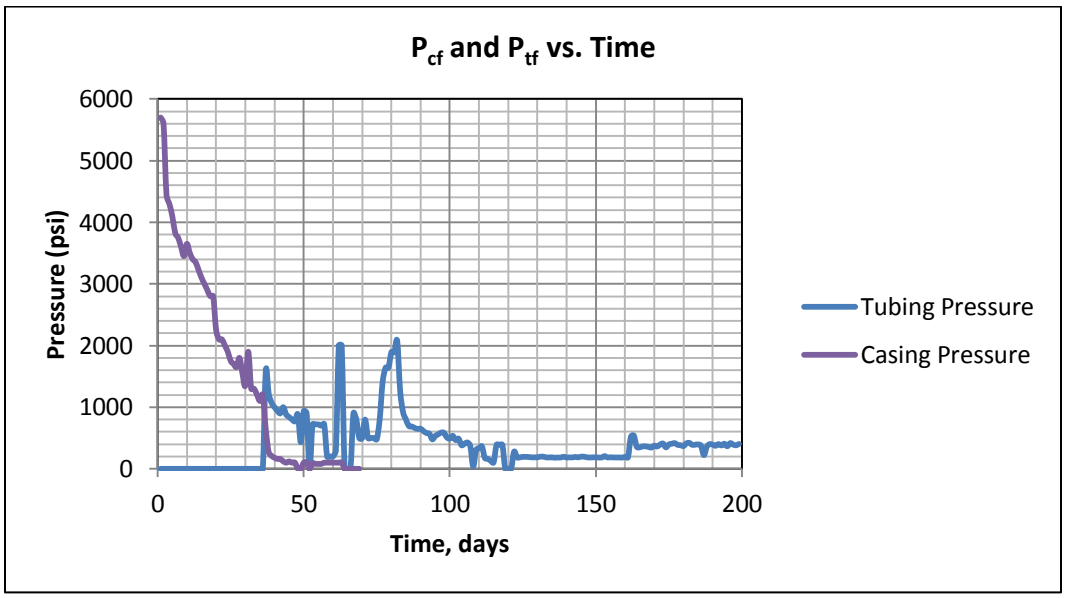

Figure 2 Well #1 p_{cf} and p_{tf} Vs Time. On days 30 to 50 the tubing and the casing were in communication, because the casing flow pressure should have been zero once the tubing was installed on day 30.

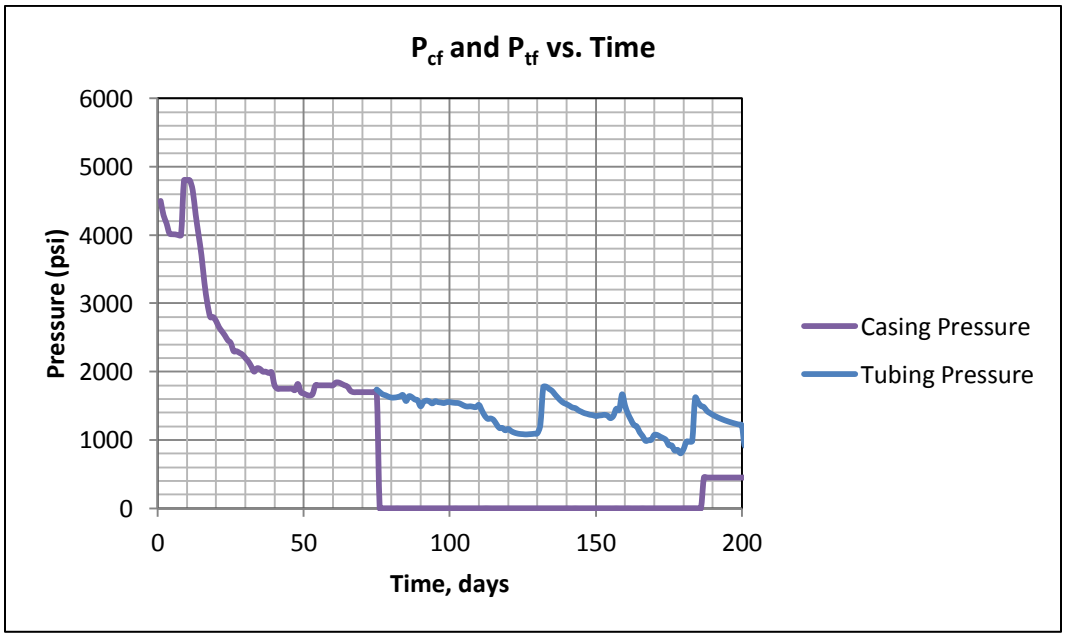

Figure 3 Well #2 p_{cf} and p_{tf} Vs Time. This is the expected behavior of pressures up to day 180, at which the casing pressure increased.

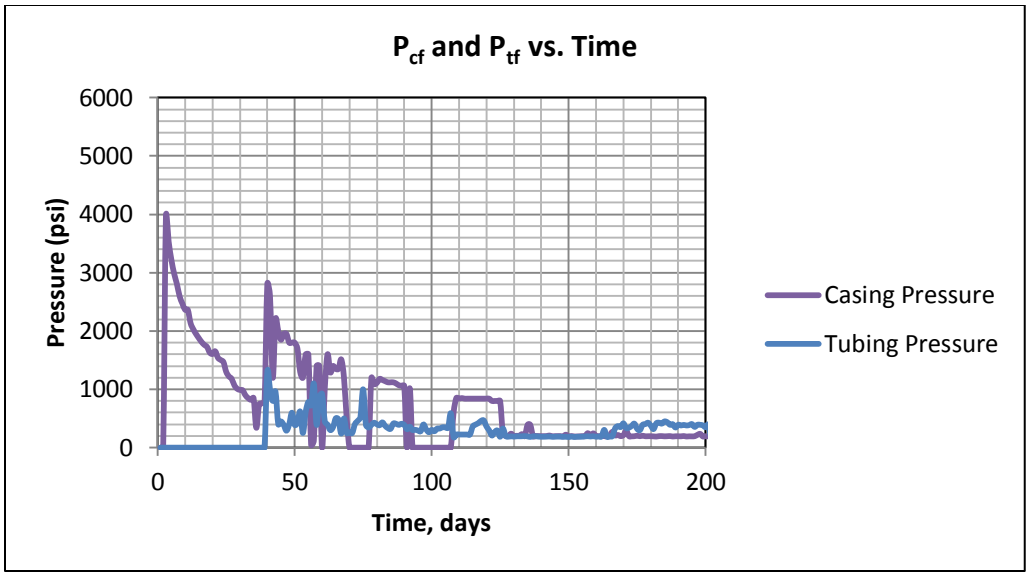

Figure 4 Well #3 p_{cf} and p_{tf} Vs Time. This figure shows that the casing and the tubing were always communicating, perhaps due to a faulty packer. Around day 40 the casing pressure increased and remained above zero for the entire remaining production time.

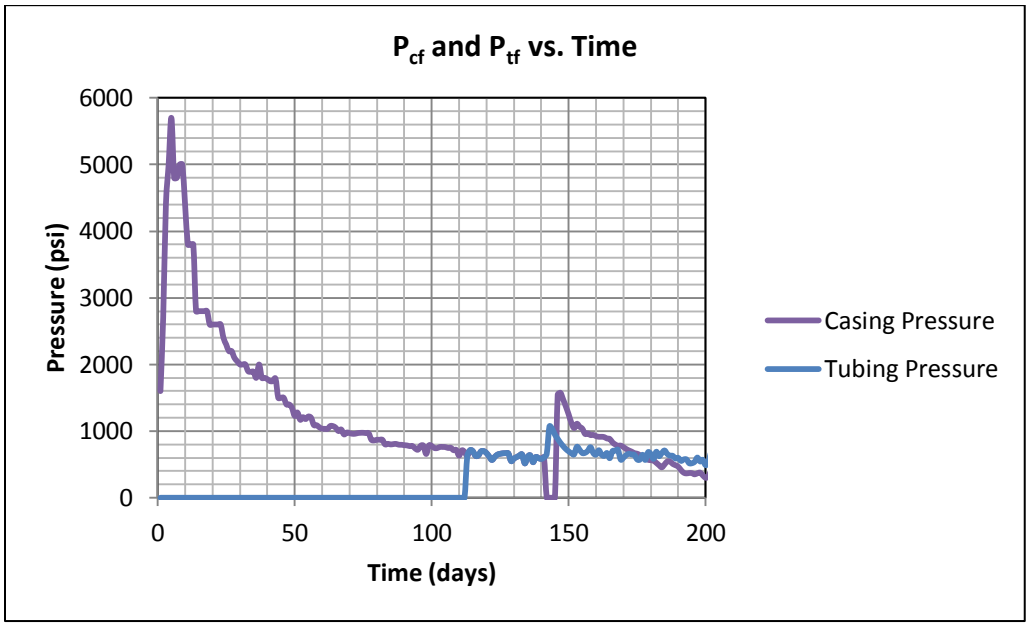

Figure 5 Well #4 p_{cf} and p_{tf} Vs Time. This figure shows that the casing and the tubing were communicating from the time the tubing was installed. The casing pressure should have been zero starting at day 110.

The operator's practice of installing tubing and not sealing it for two days was also important information to gather later, since the oil was produced through two different paths: inside the casing-tubing annulus and inside the tubing, invalidating data for two or three days.

Details such as when the well was closed, partially producing and why these events happened need to be known, located and correlated with the data set. There were many cases in which the wells were closed due to hurricane season, and events like this should be noted on the review of the well history.

Reviewing the production data is the next step recommended once pressure behavior is understood. Incompletely reported rates and incorrect allocation of rates were among the issues identified in this data set.

The oil and gas rates were plotted vs time to check for consistency, which can verify that the reported volume were correct and that they were reported at standard conditions. This may seem unimportant, but temperature at the meter can greatly affect the volume measured at the wellhead, leading to errors in rates that can percolate to the analysis later.

The oil and gas rates at a first glance seemed to correlate with each other. Water rates during fracture fluid cleanup should drop to almost zero. When negative water rates were found on the data report for two wells in the study the water rate was deemed unusable as a quantitative measurement and was considered only a qualitative indicator.

PVT properties were not provided initially, but since the values of pressures were reported at the wellhead, PVT data were requested from the operator to allow us to calculate bottom hole pressures from surface pressures.

GOR was plotted vs time for each well individually (Figure 6 to Figure 9) to check for correlation. In this step, PVT data have to be validated also or additional error will be introduced.

In this case a compositional simulation was done with the PIPESIM PVT module and the production stream was flashed twice to calculate the correct GOR at meter conditions. We entered the composition of the reservoir fluid from in the PVT report into PIPESIM. The first-stage flash was performed at 94 °F and 110 psia. Next, the liquid phase from the first step was flashed at 60 °F and 14.7 psia. PIPESIM estimated the total GOR to be 1459 scf/bbl. This value was in reasonable agreement with the value of 1429 scf/bbl calculated from the data set (Figure 10), validating the PVT data report. We could then incorporate the PVT data into the workflow with confidence.

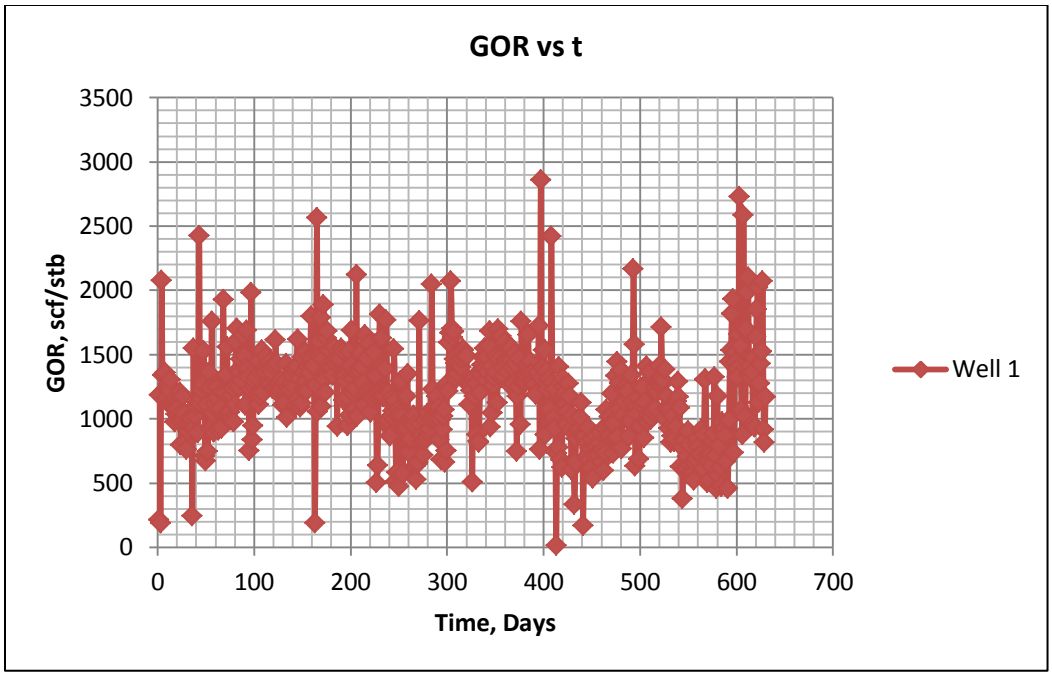

Figure 6 Well #1 GOR vs production time. This figure shows how the GOR lies between 1000 and 2000 sfc/stb

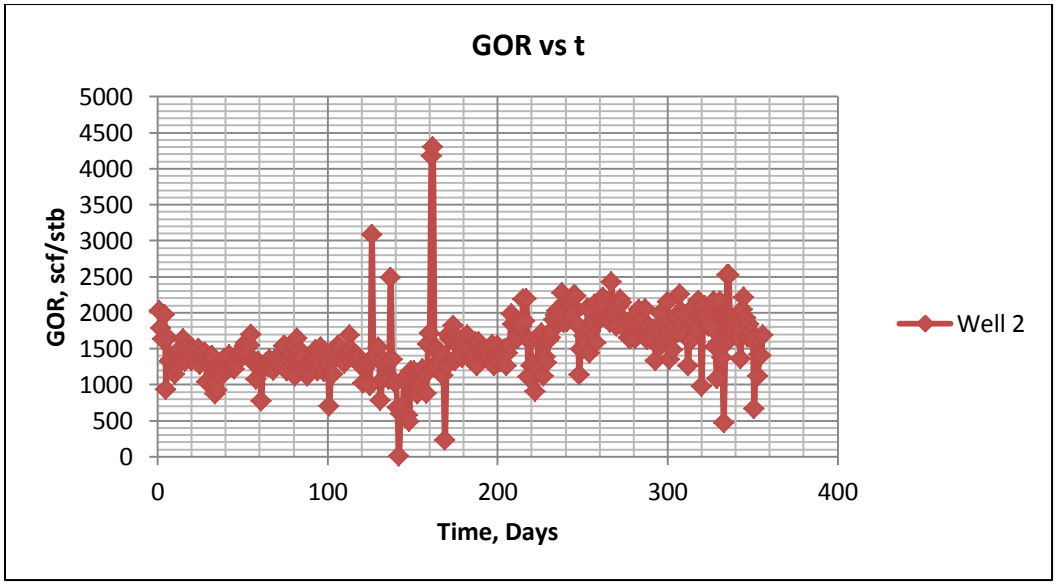

Figure 7 Well #2 GOR vs production time. This figure includes a significant outlier when the well pump was replaced at 161 days.

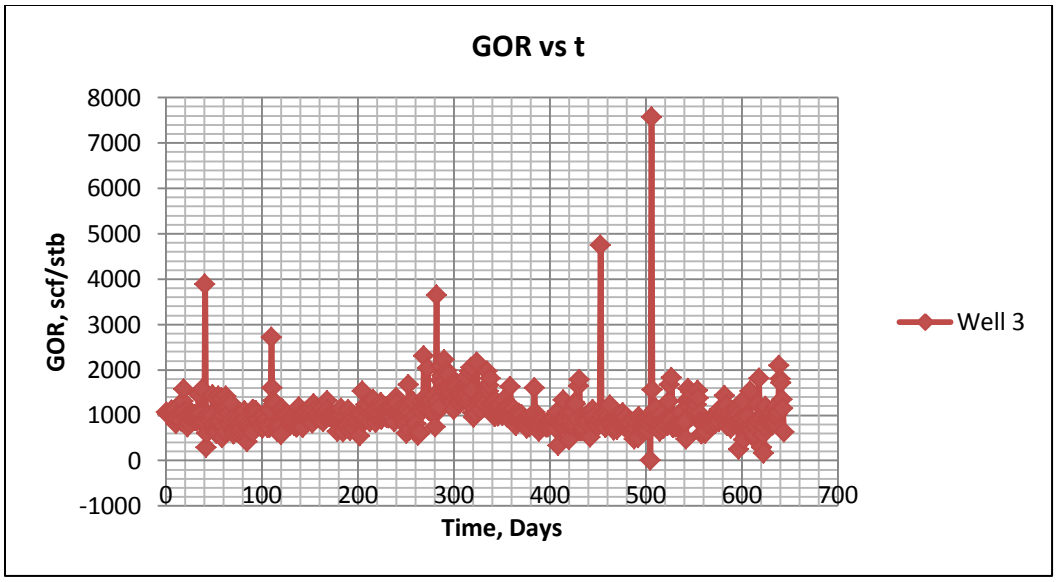

Figure 8 Well #3 GOR vs production time. Note the two successive outliers around 500 days, perhaps due to a well cleaning event.

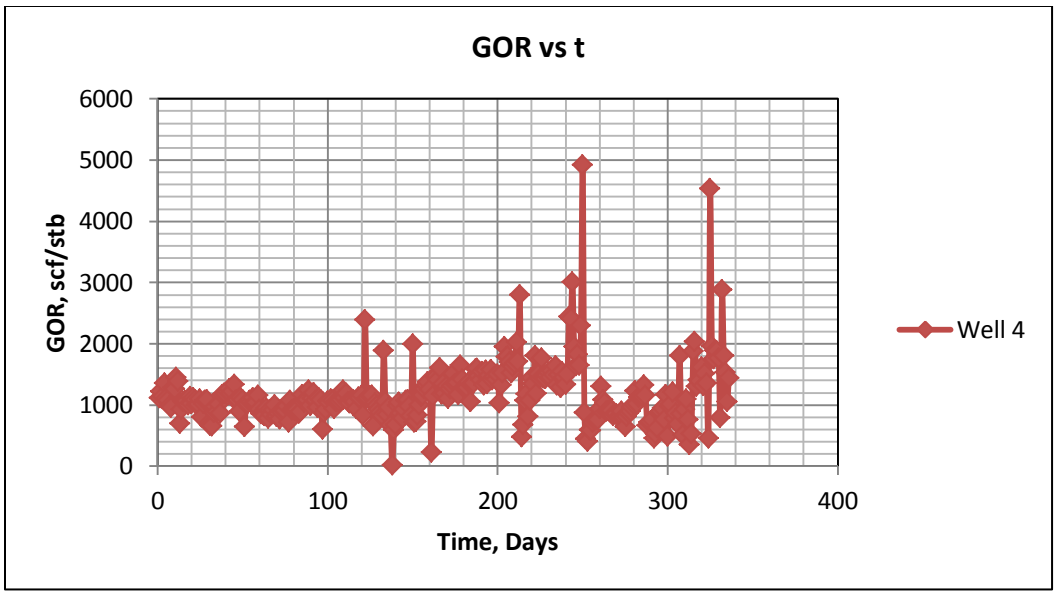

Figure 9 Well #4 GOR vs production time. The graph shows that the GOR was constant at the start of production; then it began to increase for 100 days and then decreased, correlating with a well cleanup performed 160 days after the well was put on production.

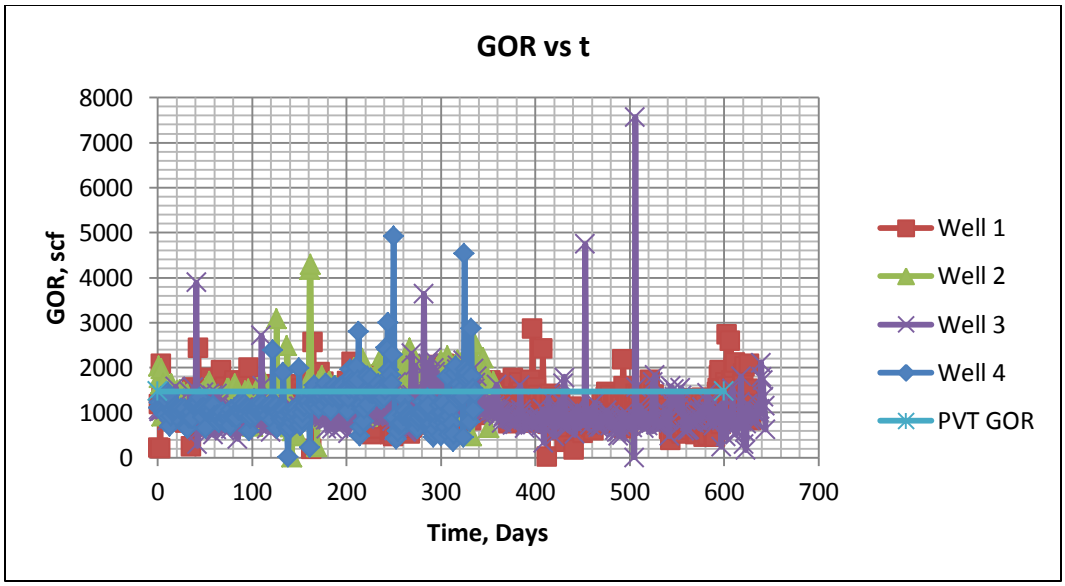

Figure 10 GOR for the 4 wells and PVT comparison. The GOR's from flash calculations based on the PVT report and the four wells agree reasonably.

STEP 2: CHECK DATA FOR CORRELATION

Ilk et. al. (2011) methodology was used for this step, it is important to remark that it is crucial that this step is followed in order to reduce the uncertainty of the data set. Pressure and rate data must correlate or the analysis should be halted and the issue investigated, or simply do not proceed with the particular data set, making the data set invalid. Simply put when pressures go up, rates should go down and when pressures go down, rates should go up. The effort and time spent on just looking at the data, way before starting any analysis will pay off on data accuracy and faster analysis.

This step when combined with the well history review can shed light to parts of the data set that can be acknowledged, modified or eliminated well before starting the analysis, and more importantly without any detrimental effects on the data set.

The diagnostics can be performed on a well to well basis or due on a group of wells that are known to come from the same reservoirs, the same field and or the same area, in order to compare it with some other group of wells. Due to the amount of data in the data set, all four wells were studied individually.

As can be seen on Figure 12 to Figure 15 every well has a data set of plots of raw and unfiltered data, this set of plots represent the history and data correlation plots. While well #1, well #3 and well #4 can be analyzed with some further filtering and data synchronization, well # 2 had a series of mechanical and completion issues that make the analysis extremely challenging, for this reason well #2 was removed from the data set. The wells for study are well #1, well #3 and well#4.

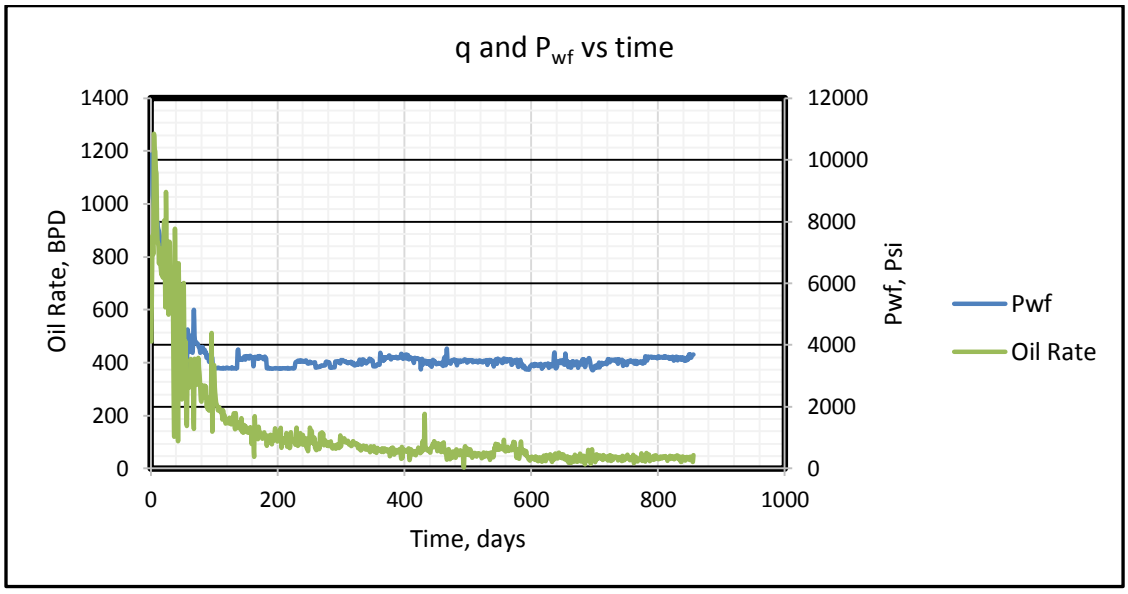

Figure 11 Well #1 q and p_{wf} vs time. p_{wf} is relatively constant over time a necessary condition for decline analysis application.

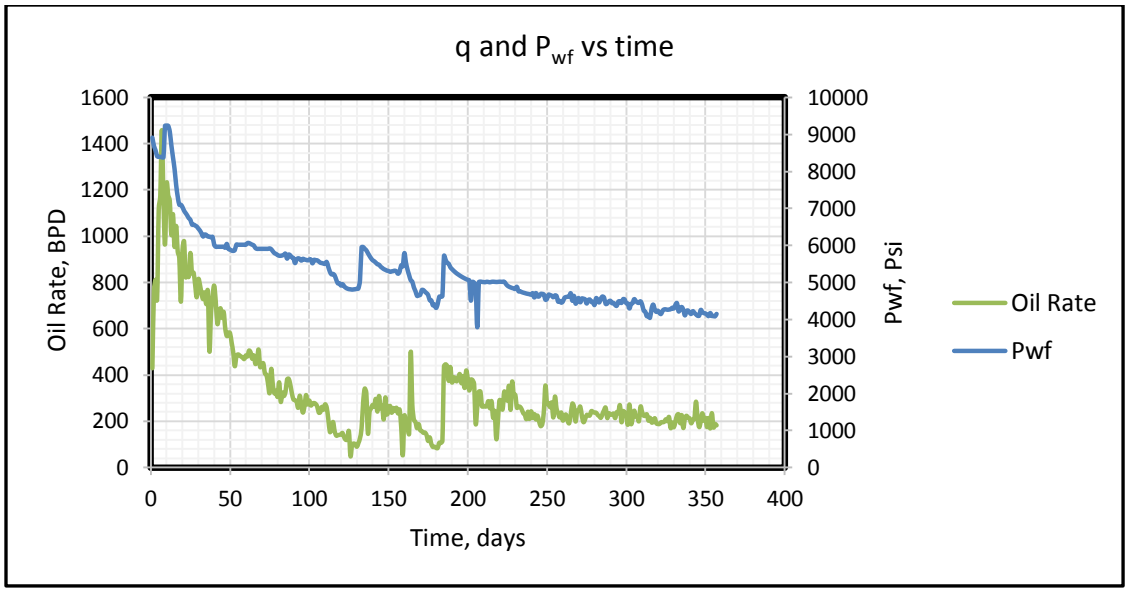

Figure 12 Well #2 q and p_{wf} vs time. It can be seen that something was majorly changed around 100 days on well 2, the pump was changed and the drawdown was affected, to the point this well is unusable for the analysis.

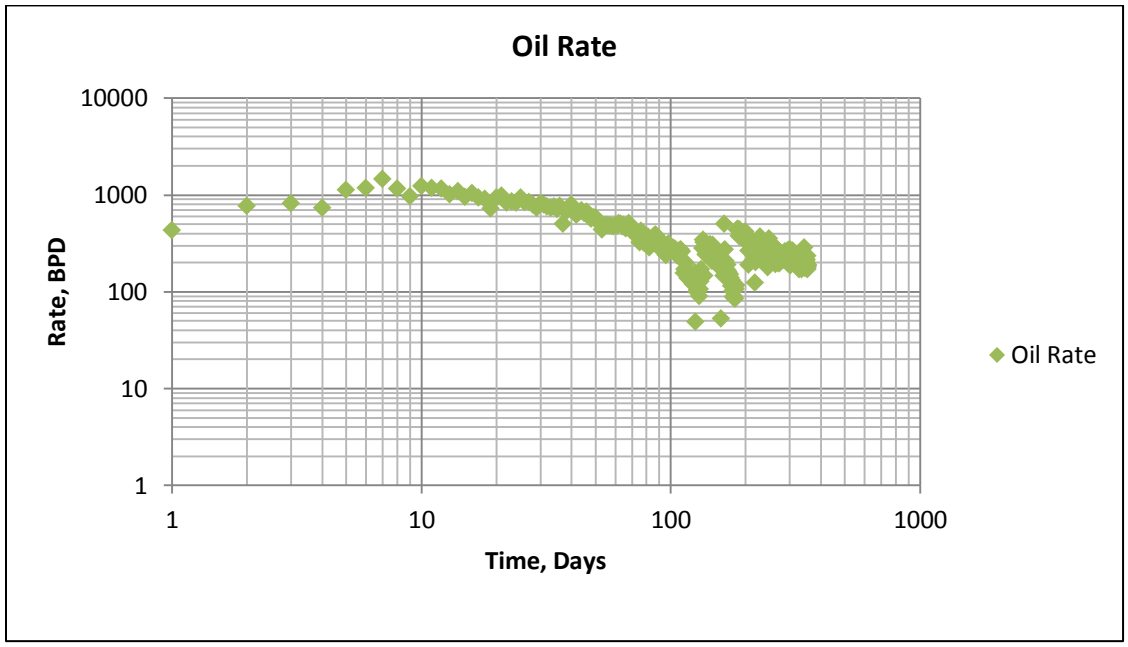

Figure 13 Oil Rate vs time for Well #2. The figure shows how the decline rate changed drastically for well #2

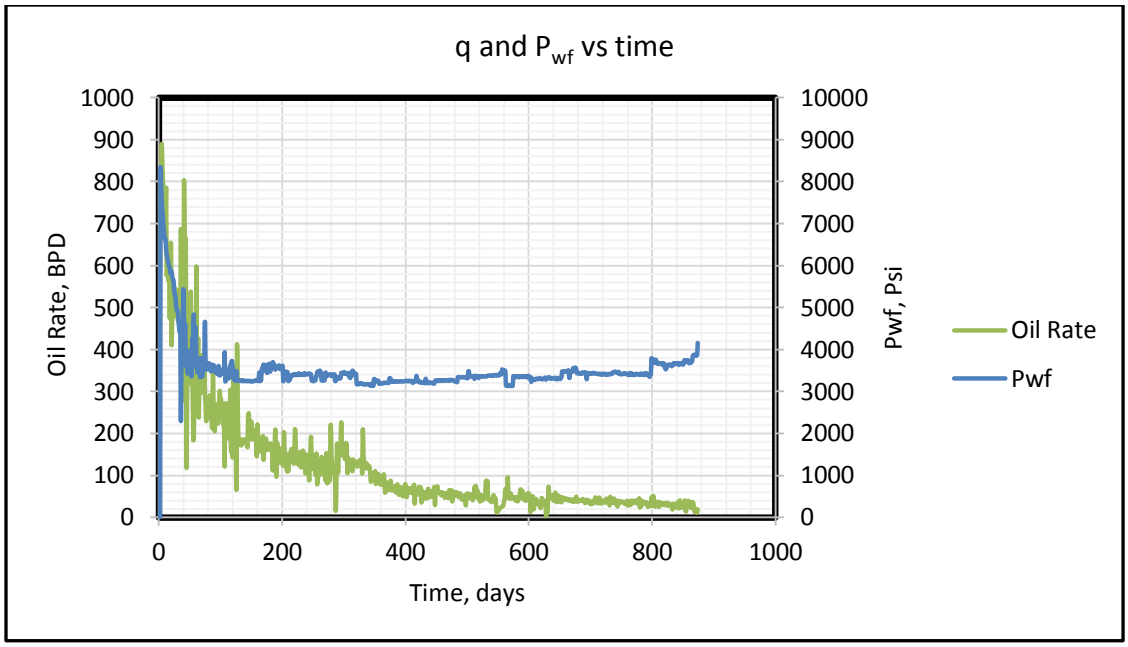

Figure 14 Well #3 q and p_{wf} vs time. There is an increase on borehole pressure at late time that doesn't correlate with the sudden decrease of oil rate, making this lateperiod suspicious of bad reporting or gauge problems.

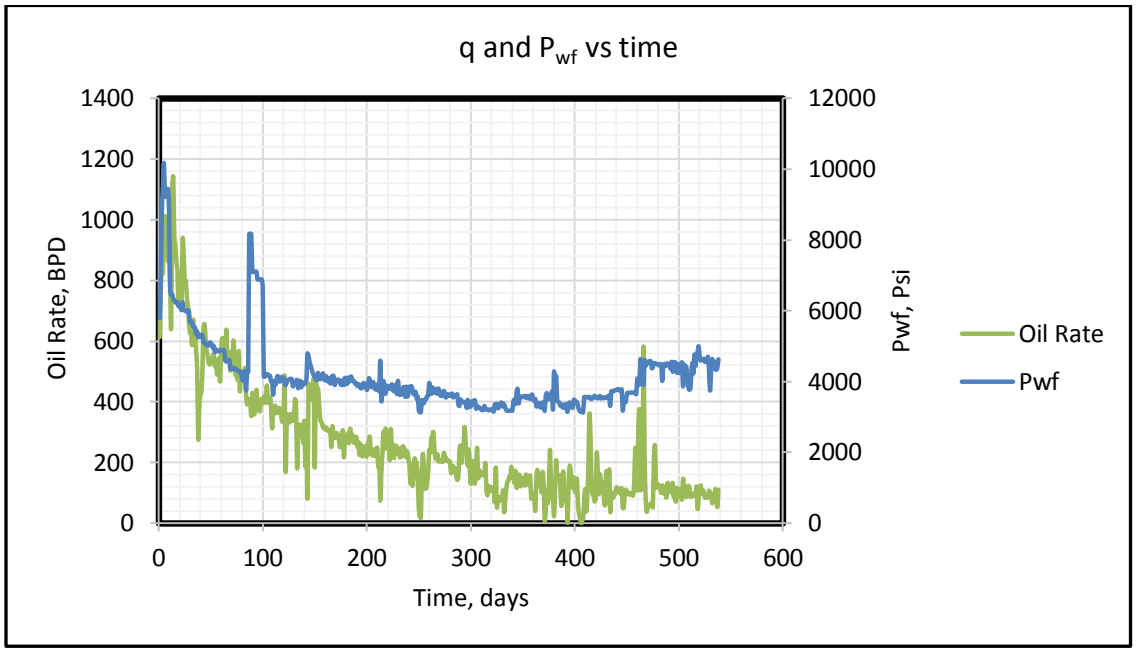

Figure 15 Well #4 q and p_{wf} vs time. This figure also shows a major event at about 450 days that altered the oil rate and had a major effect on p_{wf} without having the same effect on the rate, further revision was required for this period.

STEP 3: PRELIMINARY DIAGNOSIS

In this step, we prepare the data set for analysis. After the data is reviewed and correlated, an outlier filter proposed by Rastogi (2014) is used to smooth the data. While this filtering can be useful in lengthy data sets, in new wells with short histories the filter could eliminate data points that might be analyzed somehow with the workflow; therefore, caution is recommended when filtering small data sets.

Rastogi's methodology recommends that we assume deviations from the production data are normally distributed. Figure 16 shows that a range of one standard deviation, defined as the amount of dispersion from the average and denoted by σ, will cover +/-34.1% of the normally distributed errors. Outliers are defined as data points which lie outside the range of +1σ and -1σ from the identified data trend line.

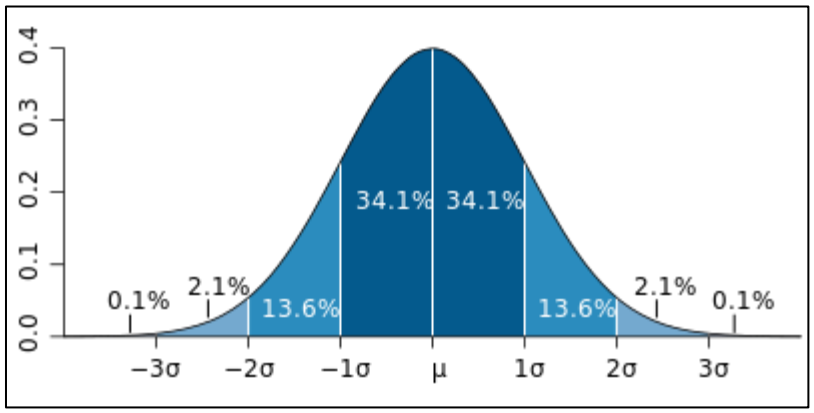

Figure 16 Typical dataset with respect to standard deviations.

The filter is used to identify the outliers and remove them while smoothing the spikes on rate and pressure vs. time plots. A fit of the data is found, using a hybrid of the YM – SEPD (Stretched Exponential Production Decline) model from Yu and Miocevic (2013) for transient flow and Arps (1945) for boundary dominated flow, we find a best fit

for the entire dataset. The SEPD model is, by definition, a transient flow model hence its applicability to the early transient flow found in all the wells in the study. The Arps decline model is designed to fit boundary-dominated flow and thus can be used for boundary dominated flow regime in our wells

First we will explain Arps' hyperbolic decline equation Arps (1945). The Arps model includes three variables: the initial rate, q_i; the initial decline rate, D_i, and a parameter, *b*, which controls the curvature of the line.

Arps (1945) noted that decline rate, *D*, in a production profile is defined as Equation 1

$$D = -\frac{\frac{dq}{dt}}{q} \tag{1}$$

Arps defined the change in the "loss ratio," 1/*D*, with time as a parameter *b* as seen on Equation 2:

$$b = \frac{d\left(\frac{1}{D}\right)}{dt} \tag{2}$$

At this point, Arps noted that, for a majority of wells that he and co-workers had analyzed, *b* was constant (unchanged with time). Assuming *b* constant, Arps arrived at the result

$$q(t) = \frac{q_i}{\left(1 + bD_i t\right)^{\frac{1}{b}}} \tag{3}$$

As Lee (2012) pointed out Arps' decline models have met the test of time: they have been applied successfully (when the conditions required for their applicability have been satisfied) for almost 70 years. We noted that Arps observed that most of the

production profiles for most of the wells that provided the basis for his decline models exhibited values of b that did not change with time.

Next, we will explain the SEPD model (Valko et. al 2010). The SEPD model can also be used to forecast production rates, based on the following equation

$$q = q_o \times exp[-\left(\frac{t}{\tau}\right)^n]. \quad (4)$$

We construct a log-log plot of $\ln\left(\frac{q_o}{q}\right) vs\ time$, suggested by Yu and Miocevic (2013). Here q_o is the initial production rate, conveniently assumed to be the highest rate observed in history. Based on the straight line fit of the plot, we obtain the value of n. This is calculated by representing the equation of the straight line on the plot in the form

$$y = (int)x^n. \quad (5)$$

In the equation (5), int is the intercept and the exponent of x is n. The value of τ is calculated from

$$\tau = \exp[(-\ln(int))/n]. \quad (6)$$

Once the values of $\tau\ and\ n$ are obtained, the SEPD model can be used to forecast production rates from equation (4). This equation will be used to forecast rates until the end of transient flow, after which switch from YM-SEPD to boundary dominated flow will take place

The end of transient flow, almost always transient linear flow, is the time (t_{elf}) obtained visually after applying the procedure recommended by Chen (2000) and Anderson and Mattar (2003). These authors suggested by log q vs log t and log q vs log

MBT (material balance time, cumulative production/rate) for the unfiltered data. This particular procedure will be explained in more detail in step 4.

After the end of the transient linear flow is identified and the boundary dominated flow has begun, we apply the Arps model, for which we must assume a value of decline exponent b. As Okuszko et al. (2005) predicted, shale gas wells producing at the highest possible drawdown will show b values approaching 0.5. Based on these transient and boundary-dominated flow regime trend lines, the outliers are identified as points which lie more than one standard deviation from the lines.

For the Well #1 data set a value of q_o=1300 stb/d was used and the values of n and int, were found using the procedure suggested by Yu and Miocevic (2013) as seen in Figure 17. These values were used to construct the SEPD curve. The same procedure was followed for wells #3 and #4 as shown on Figure 19 and Figure 21. The t_{elf} was obtained manually for all three wells, after plotting log q vs log t and log q vs log MBT as shown on Figure 18 and Figure 23. Once this time was found, the decline model was switched to the Arps model. For each well in the data set, sensitivities for the b value were run; for well #1, the values were b=1, b=0.5 and b=0.2. The value of b=0.5 best fit the data as predicted by Okuszko et al. (2005). Figure 18 shows the match. For Well #3 a value of q_o=889 stb/d was selected and the values of b=0.5 and b=0.8 were used to assess the sensitivities, with b=0.5 proving to be the better choice (Figure 20). For Well #4 a value of q_o=1100 stb/d was used and Arps's exponent value of b=0.5 was also used as seen on Figure 22.

Once the outliers are identified as points which lie outside one standard deviation from the chosen trend lines, these points are removed from the analysis. While the original method suggested a second pass with the filter, since the data set was not extensive, we decided to use only one pass. The filter was applied only to rates and not to pressures, remembering that maintaining correlation between the two is critical for data analysis.

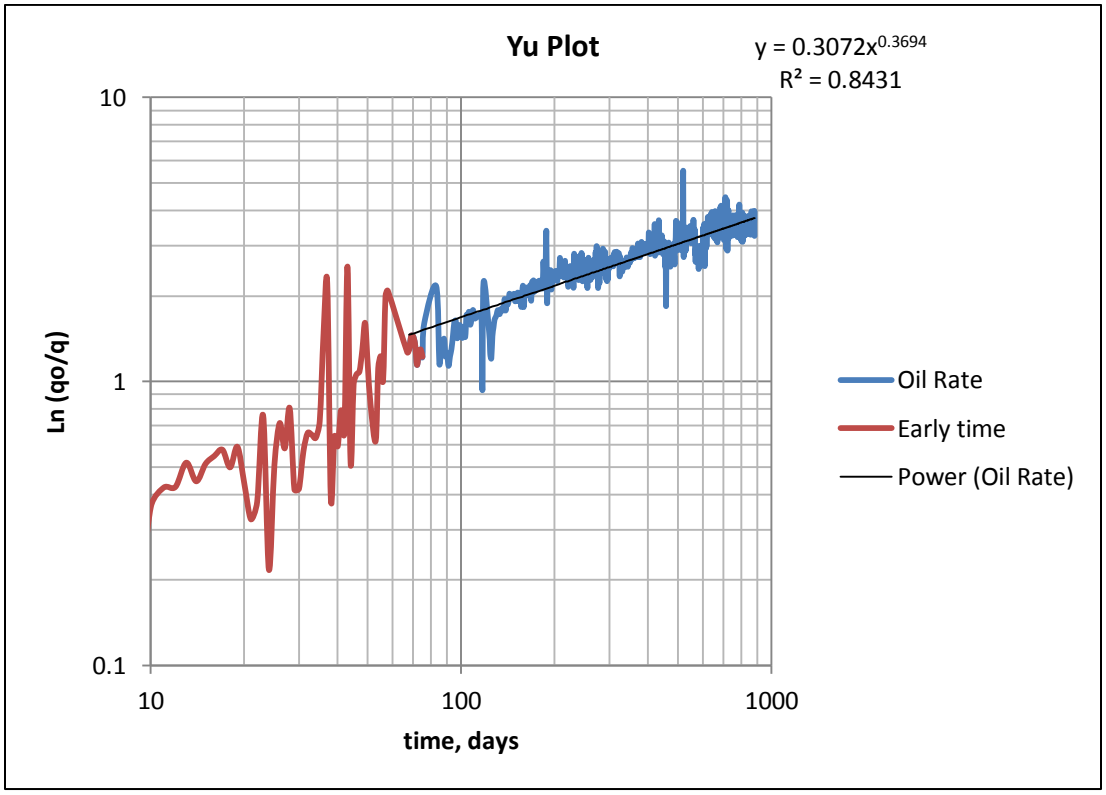

Figure 17 Yu Plot for Well #1. This figure shows that the early time data do not lie on the linear trend line fitting the later data.

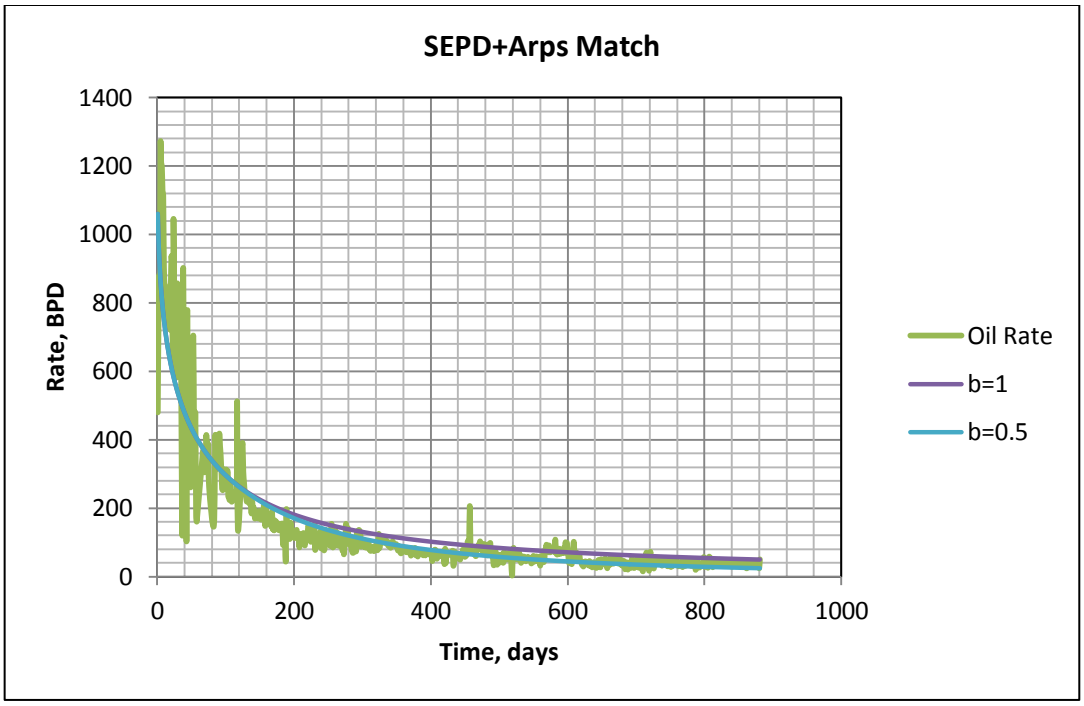

Figure 18 Model matching Well #1. Of,the different *b* values, *b*=0.5 provides the best fit during for the late time period.

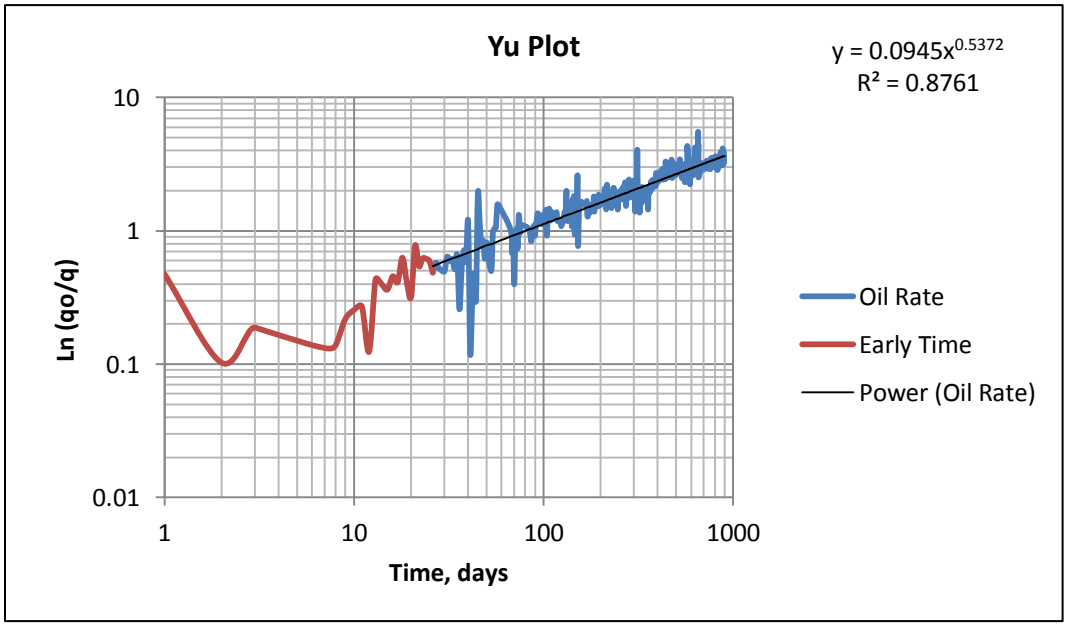

Figure 19 Yu Plot for Well # 3. Early data do not fall on a linear trend, hence these points are excluded from the regression used to find the model parameters.

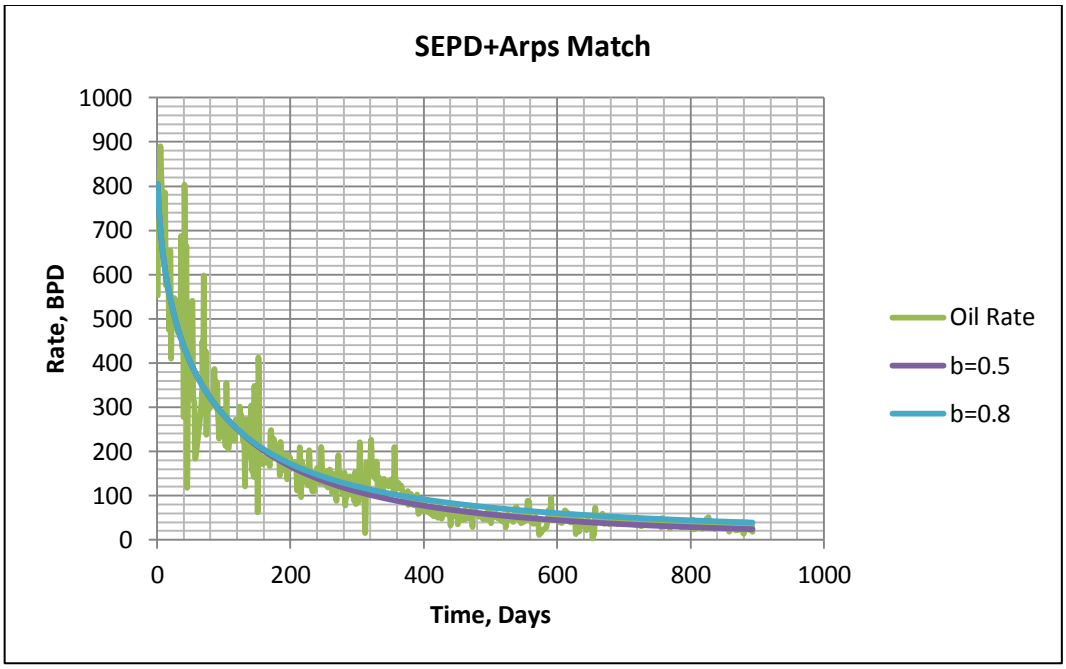

Figure 20 Model matching Well #3. The sensitivities were ran for different *b* values and *b*=0.5 was optimum.

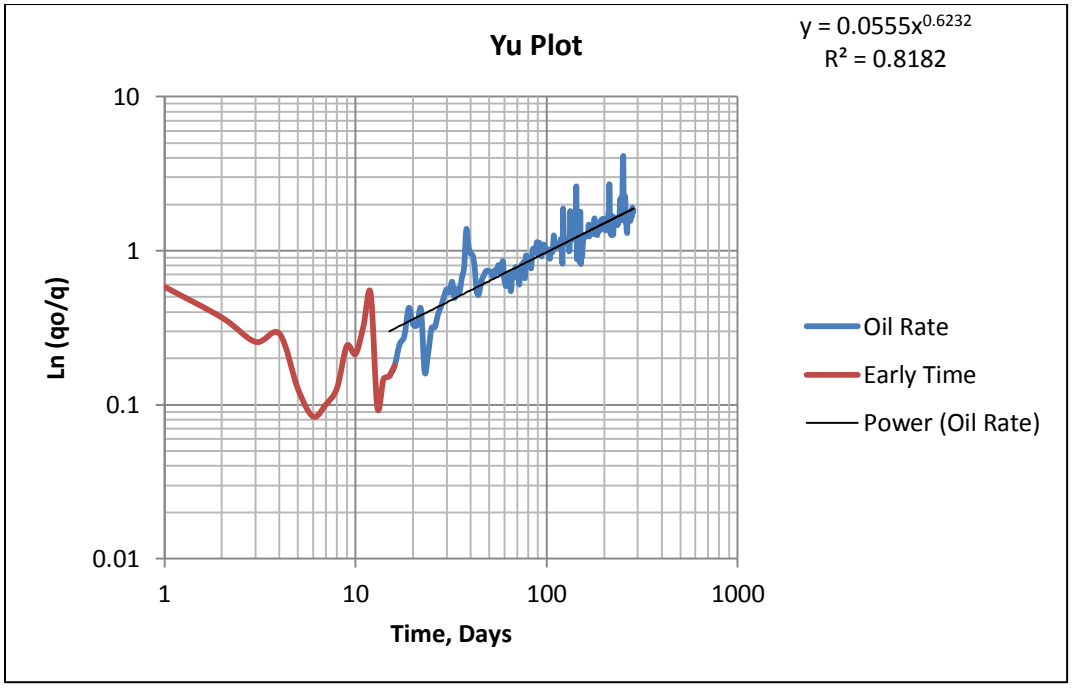

Figure 21 Yu Plot for Well # 4. The figure shows that about 20 days of the cleanup period and initial production were removed from the data correlation for the Yu plot.

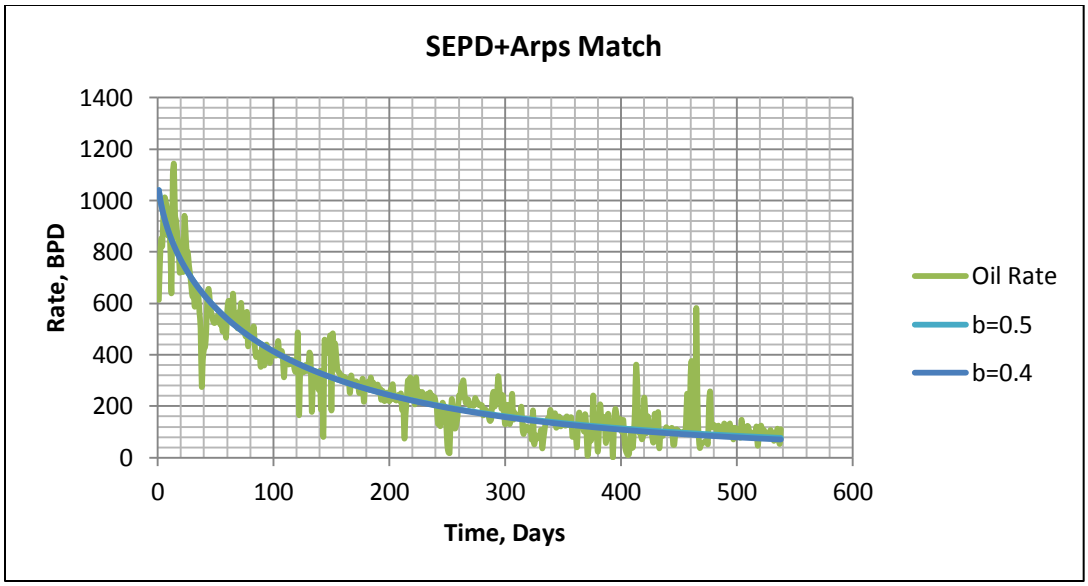

Figure 22 Model matching Well # 4. Sensitivities were run for the *b* values and a value of *b*=0.5 was optimum.

Figure 24 shows how the data set looks after the filter is applied. The preliminary diagnostics plot can be cleaned up easily and the data trends can be visualized clearly.

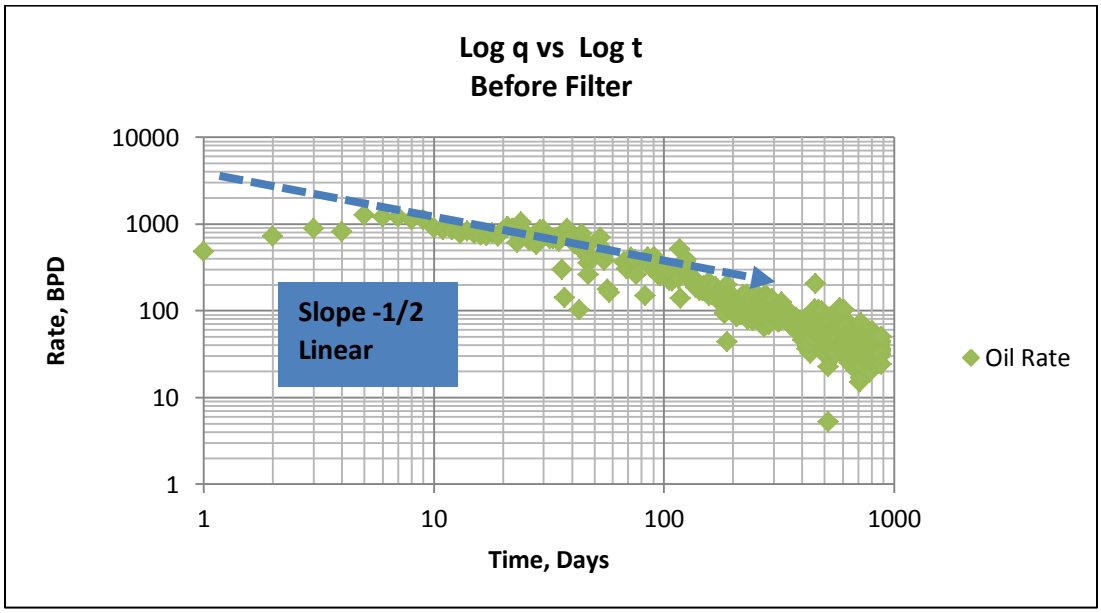

Figure 23 Well #1 before filtering. The figure shows how badly the data scatter how the flow regime identification can be hindered by this scatter.

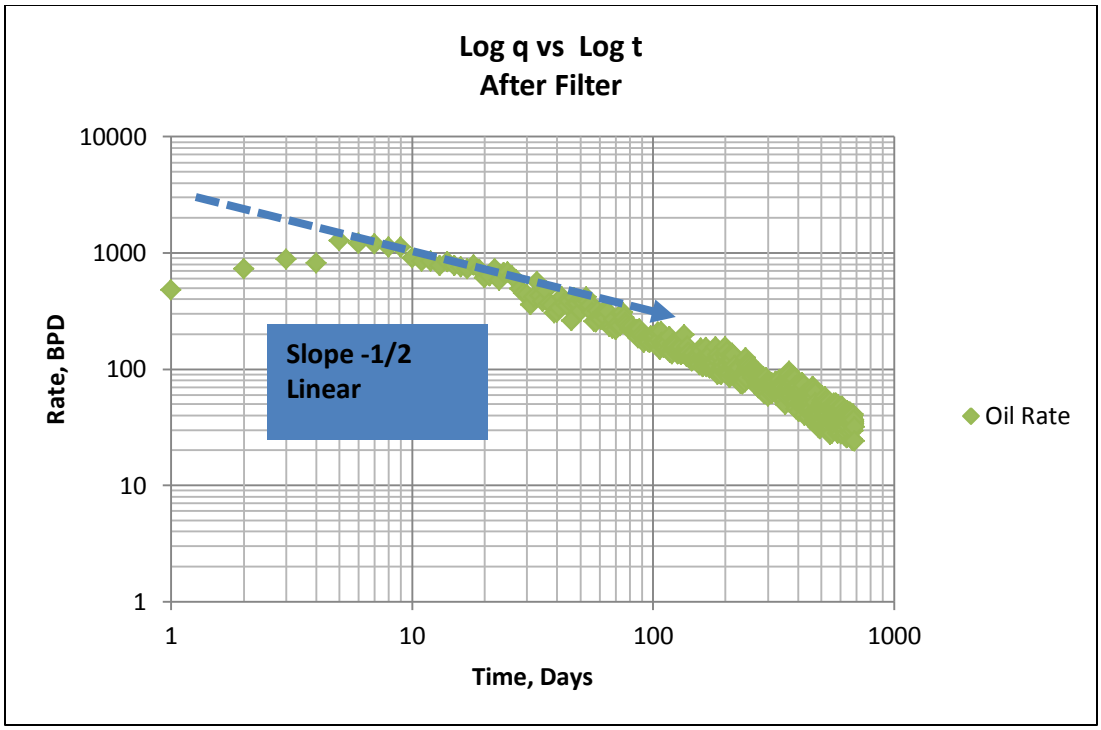

Figure 24 Well #1 after filtering in comparison to Figure 23 the scattering is diminished and the flow regime identification is clearer.

STEP 4: FLOW REGIME IDENTIFICATION

In this step, we identify flow regimes in the historical production data. Several authors have studied flow regimes in horizontal wells with multiple transverse fractures including Song and Ehlig-Economides (2011) and Clarkson et al (2009). They have pointed out that the two regimes that may be predominant are early transient linear flow, attributed to the flow from the reservoir to the fractures, and a boundary dominated flow regime after the fractures interfere with one another. We may also see a second transient linear flow regime if flow from outside the Stimulated Reservoir Volume (SRV) occurs to a meaningful extent.

This could be the most critical step in the workflow. The literature suggests several methods to identify flow regimes; based on the procedure proposed by Lee (2013) the following plots were used: log-log plot of hydrocarbon rate vs time, pressure-drop normalized hydrocarbon rate vs time, hydrocarbon rate vs material balance time, and pressure-drop normalized hydrocarbon rate vs material balance time.

We expect a fracture-fluid clean-up period, which is identified by decreasing water rate and off-trend oil rate. This period of the production history should be excluded from the flow regime identification step. When pressure data are available, the use of normalized rate data is encouraged, and the times at which the pressure data do not correlate with the production data should be investigated and later excluded if nothing can be done to improve the data quality.

Chen et al (2000) noted that if we plot of $\frac{q}{(p_i - p_{wf})}$ vs. time on a log-log graph, we obtain the shapes in Figure 25 during transient flow (upper left) and boundary-dominated flow (BDF, lower right), with the parameter on the lower right being Arps' *b*-factor:

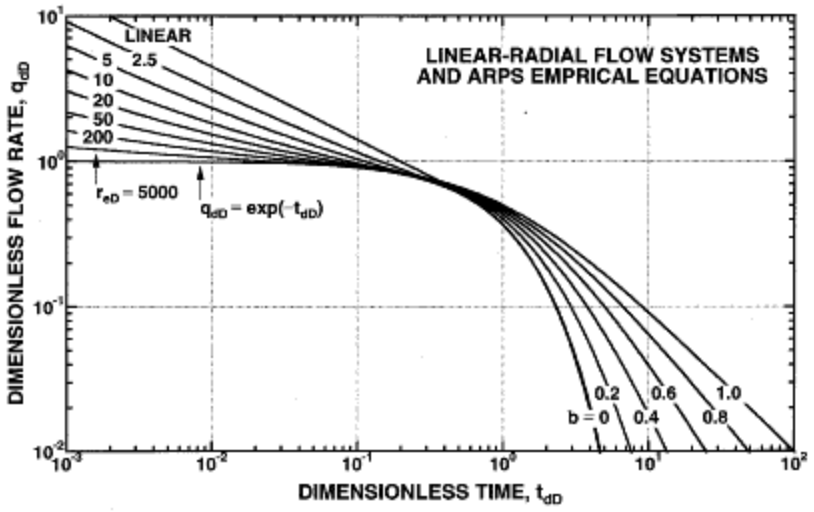

Figure 25 Chen's modification of the classic Fetkovich type curve. Arps' *b*=2 correlates with -1/2 slope during the transient linear flow regime (early times, upper left). During boundary-dominated flow (lower right) a family of curves that are all concave downward appear. (After Chen (2002)).

As Lee et al (2003) mentioned, none of these lines during BDF have a slope of exactly negative unity, as is sometimes assumed to be diagnostic, and which some consider required to positively identify boundary-dominated flow. However, each curve has a slope that is concave downward; this is the characteristic influence of boundaries. The smaller the *b*-value during boundary-dominated flow, the steeper the slope becomes with increasing time. During transient linear flow, the log-log plot is a straight line with a slope of -½. A lengthy transition region may appear between transient linear flow (or transient radial flow or bilinear flow in some cases) and boundary-dominated flow.

The rate or normalized rate vs. MBT plot was first introduced by Blasingame (1986), and he was able to show that the boundary-dominated flow equation for variable-rate production could be written in a form similar to Arps' hyperbolic flow model (b=1) if we replace actual time in the flow equation with MBT. Later Anderson and Mattar (2003) explained that MBT transforms normalized pressure or rate data gathered from a

well produced at constant BHP to the equivalent data that would have been obtained had the well been produced at constant rate. Lee et al. (2013) stated that this plot is among the most powerful tools that we have available for flow regime identification.

As Clarkson, (2013) recommended, flow regime identification should be done in parallel or after well completions, surveillance, geological, microseismic or any other field data is appraised to more accurately identify flow regimes.

In this study, all the data used in the workflow were filtered data. Figure 24 and Figure 26 are log-log plots of oil rate vs. time and oil rate vs. material balance time for well #1. In the figures and as predicted in the literature reviewed, two regimes were clearly identified: early transient linear flow and late boundary dominated flow. This information must be taken into account in the rest of the workflow because it will have important implications on the analytical model to be chosen in step 7.

The same plots and procedure were followed for well #3 and well #4. Figure 27 to 30 show that the wells have similar decline characteristics and that flow regime identification is clearer after the outliers are removed. When production data from all three wells are plotted in Figure 31, we see that they have similar flow regimes. To make this comparison meaningful and unbiased, the rate had to be normalized by lateral length; otherwise, true well behavior could be masked. This is important in this data set since t well #4 is almost 50% longer than wells #1 and #3.

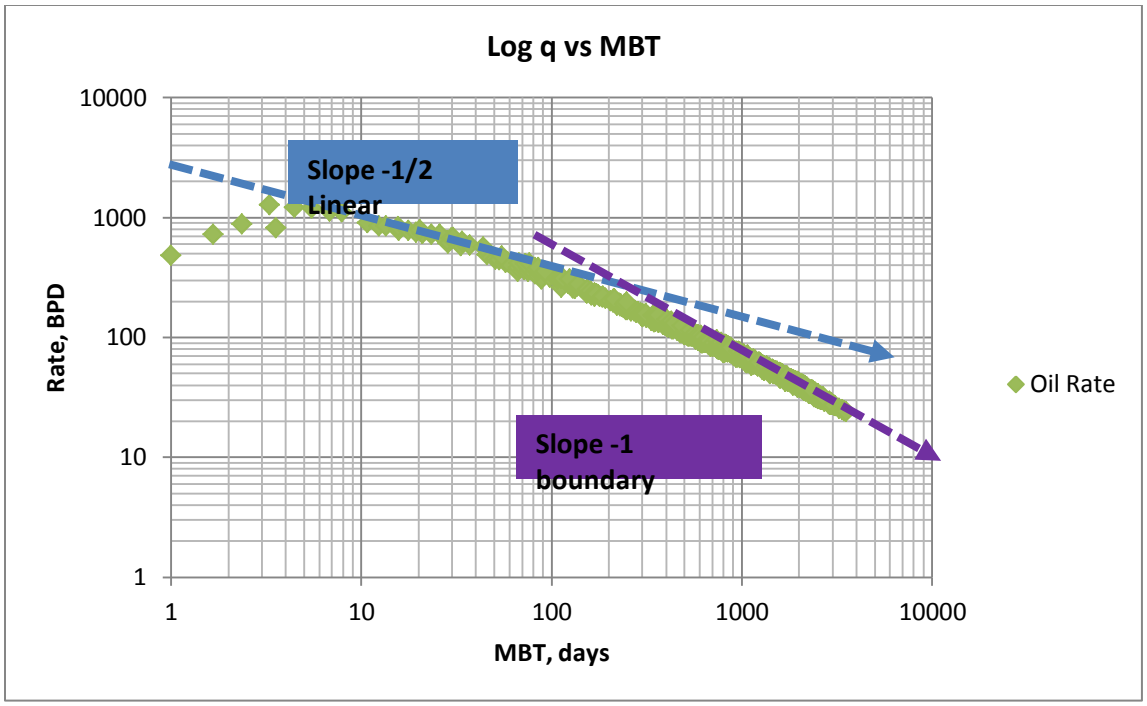

Figure 26 Log q vs. log MBT for well #1. Slopes of -1/2 and -1 allow us to identify unequivocally the start and end of the flow regimes.

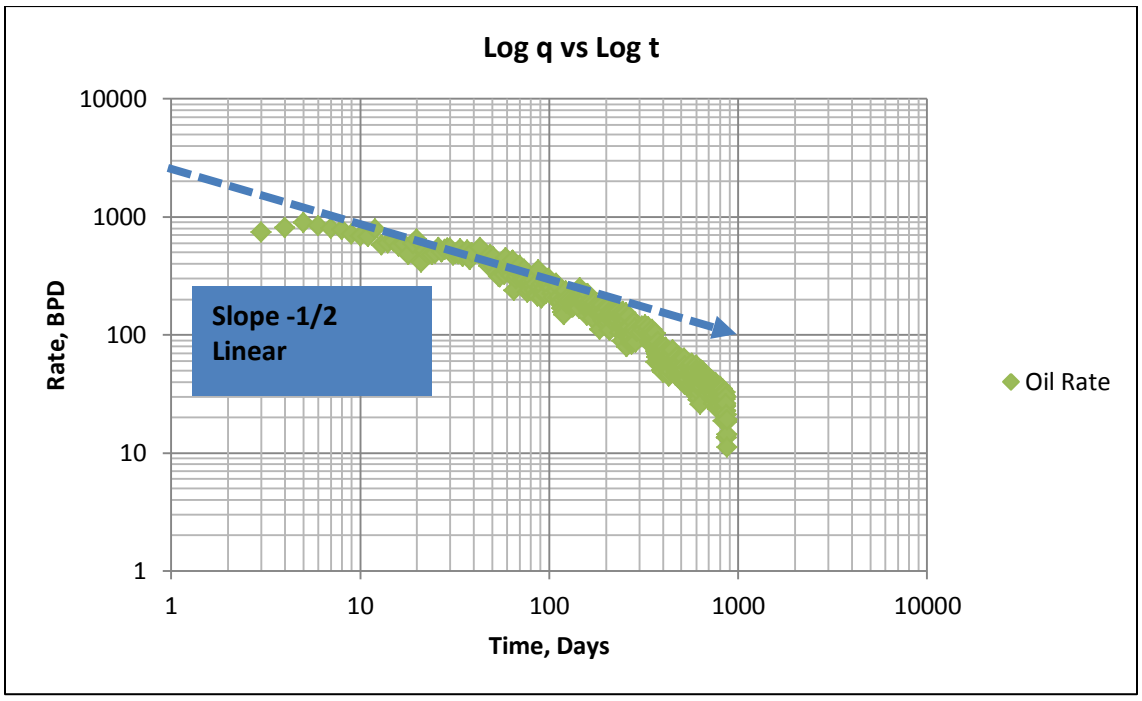

Figure 27 Log q vs. log t for well #3. The figure shows how the early data deviates from the linear flow as expected and how much clearer after the filter is applied the flow regime identification is.

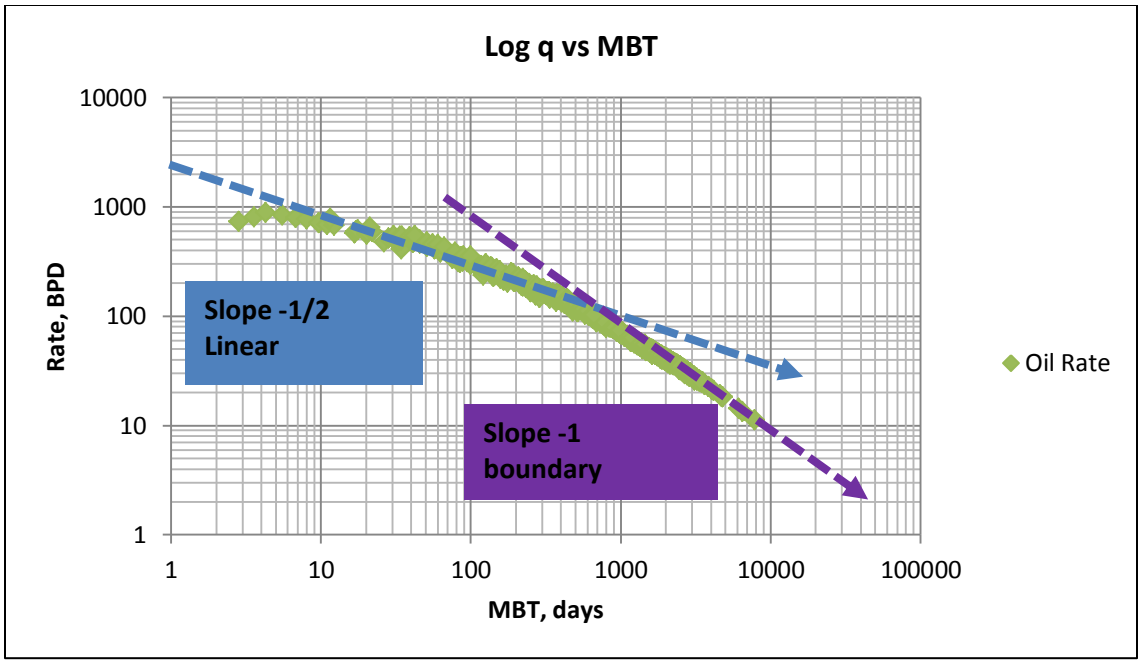

Figure 28 Log q vs. MBT Well #3. The figure shows that around 40 MBT days the slope of -1/2 becomes more evident, probably due to fracture clean up. The boundary-dominated flow regime is more clearly identified than in other wells is the study.

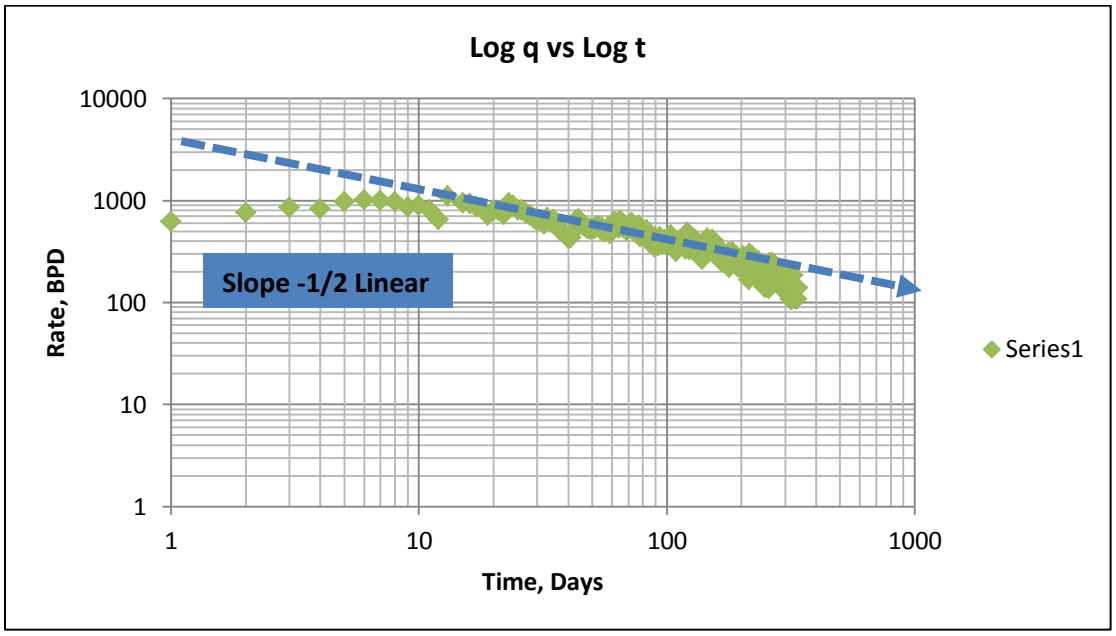

Figure 29 Log q vs. log t Well #4. The figures shows clearly that the early time rate data do not match any simple flow regime. The boundary-dominated flow regime appears but more production data would be necessary to refine the flow regime identification at later times.

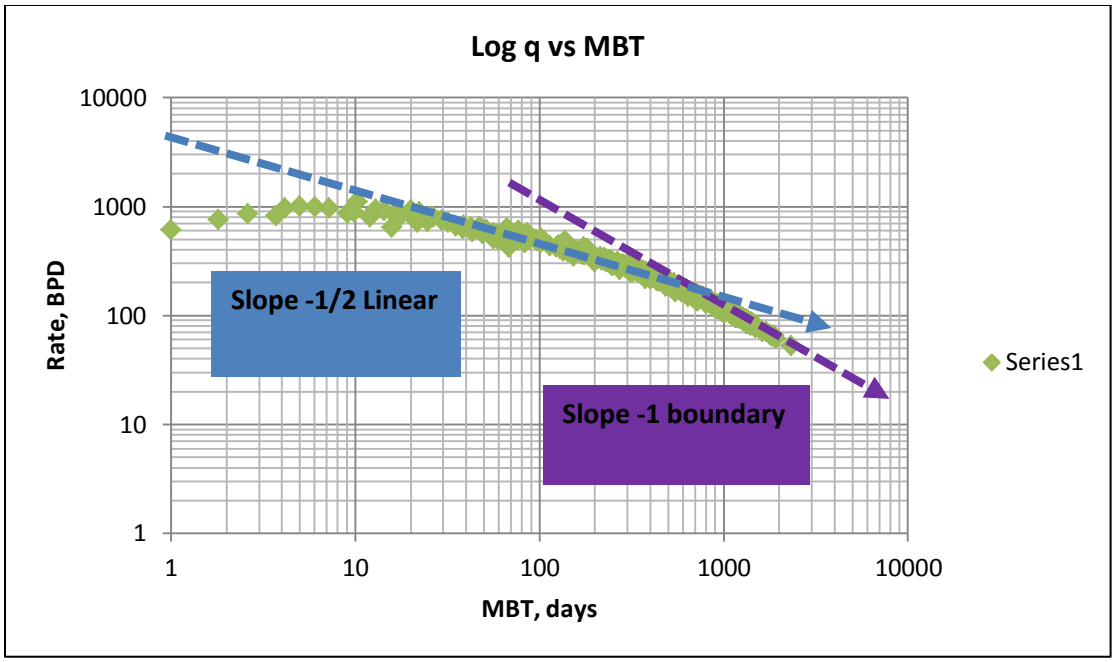

Figure 30 Log q vs log MBT Well #4. Once again the MBT plot is a more useful and explicit indicator of where the flow regimes appear in the data. Boundary-dominated flow is clearly present in the latest data.

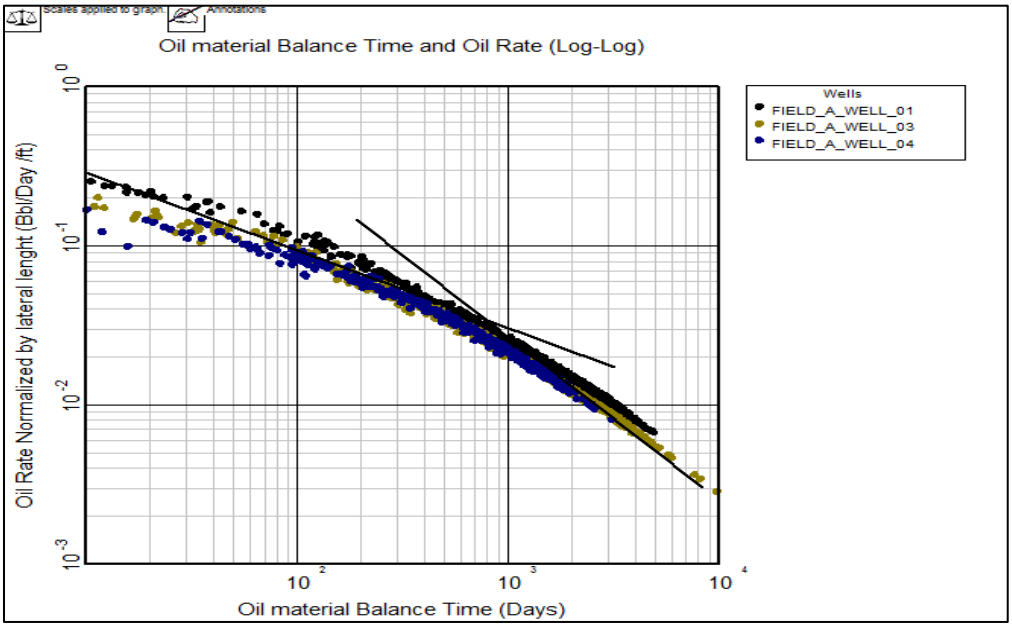

Figure 31 Oil rate (normalized by lateral length) vs. oil MBT. This figure shows clearly that once the rates are normalized by lateral length all 3 wells have similar behavior in the linear flow regime and in the boundary-dominated flow regime.

Figure 32 shows that well #4 appears to perform better than the two other wells. A feature of the KAPPA Citrine software that we used in this phase of the work allows us analyze this behavior more definitively. This feature allows us to organize wells by work group. KAPPA Citrine software permits the rapid loading of mass public, client or simulation sources for the processing of multiwell data. Using visualization, trend identification, and multiwell comparison, the user can fully understand and interpret field performance using diagnostics and decline curve analysis. Citrine can transfer single well data to KAPPA Topaze NL (another module in the KAPPA software package), retrieve the analytical or numerical forecast from Topaze NL and use it as a seed for a single or multiwell analysis and forecast. KAPPA Topaze NL is reservoir production software suited for rate decline analysis, with a wide range of well, reservoir and boundary models. Topaze NL can simulate bottom-hole pressures given rate data. Production history is matched is using nonlinear regression of pressure, rate, cumulative production or any weighted average compared to a proposed well and reservoir model. Topaze NL integrates additional specialized plots and substantially enhanced analytical and numerical models, especially adapted to the low permeability range of unconventional formations. In step 6, we used this software to match the field data to the analytical models we selected.

It can be misleading to think that well #4 is a better performer than the other two wells, when we compare only cumulative oil production. Expertise and a close look at the data in Figure 33 can prevent a gross error. The industry is still selecting well lateral length by trial and error, and sometimes the lateral length has nothing to do with the reservoir and has everything to do with lease permits and other factors. Due to these

variables, normalization by lateral length is strongly recommended. Note that Figure 32 and Figure 33 were generated using the KAPPA Citrine software.

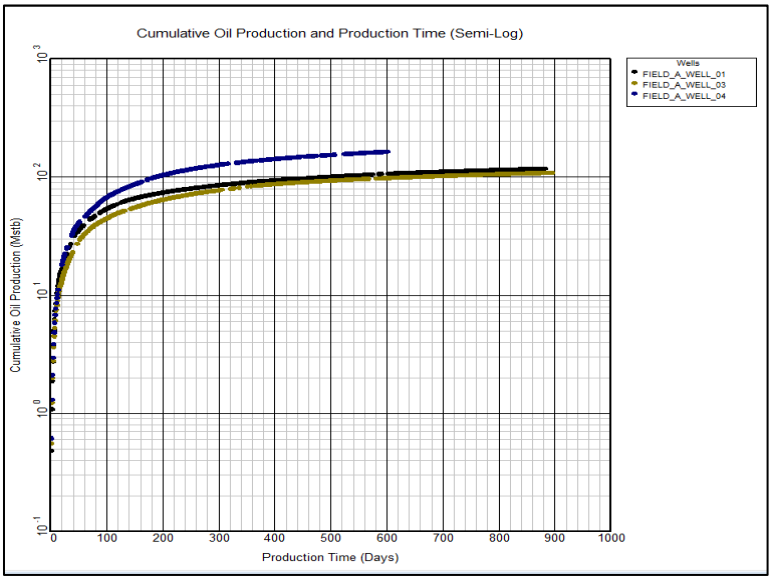

Figure 32 Comparison of cumulative oil production vs. time for wells #1, #3 and #4. If no lateral length optimization is applied, well #4 appears to perform better than wells #1 and #3.

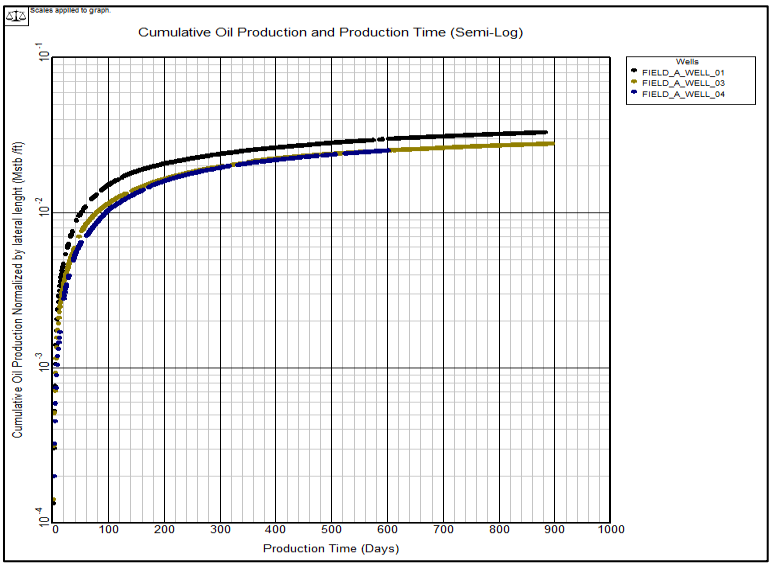

Figure 33 Comparison of cumulative oil production vs. time for wells #1, #3 and #4, with production data normalized by lateral length. When the data are normalized we see that the behavior shown in Figure 32 is due to the masked effect of lateral length. Well #1 is actually the best performer of the three wells.

After we normalize for lateral length with Citrine, we see that the three wells are quite similar, and well #1 is a more efficient producer than the other two wells. An additional plot of productivity index vs. time in Figure 34 also compares all three wells. Figure 34 confirms that the wells behave in similar ways, important to know because the completion procedure was the same for each well. Conclusions reached from a study of one of the wells may then be applicable to other wells in the group.

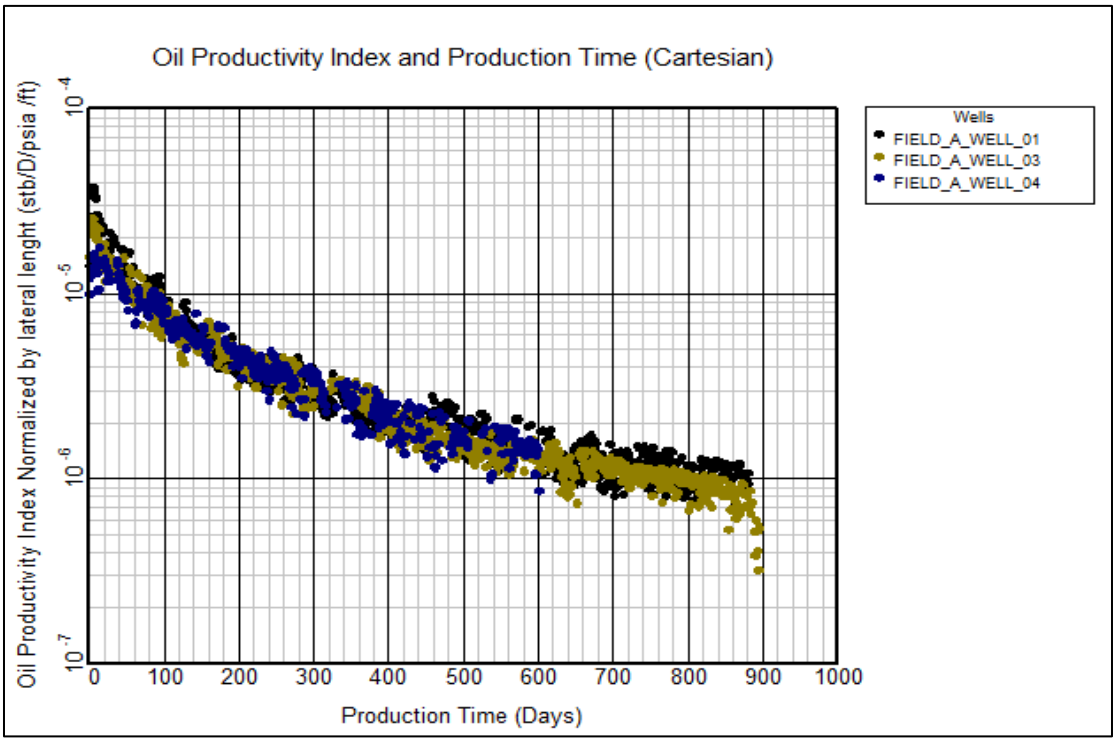

Figure 34 Oil productivity index vs production time. Once the cumulative production is normalized by lateral length, the productivity index is about the same for all three wells.

STEP 5: STRAIGHT LINE ANALYSIS

If $\frac{p_i - p_{wf}(t)}{q(t)}$ versus $t_{mb} = \frac{Q(t)}{q(t)}$ is plotted on a log-log scale the boundary dominated flow will exhibit a unit slope line, similar to constant rate data in the pseudo-steady state flow regime. Also, if we take the derivative of the normalized pressure with respect to the

logarithm of t_{mb}, we can identify flow regimes with even more confidence. Unfortunately, the noise level in the derivatives is usually too high for further analysis. One workaround is to use a normalized pressure integral, in a manner analogous to the Palacio-Blasingame type-curves (Palacio and Blasingame, 1993). The integral preserves the signature of the flow regimes and can significantly reduce the noise in the data.

As Song and Ehlig-Economides (2011) noted, when both linear and boundary dominated flow regimes appear on the rate normalized pressure vs. material balance time plot, both permeability and the average half-length of created fracture can be estimated. This is another reason why it is so important that flow regimes are accurately identified; otherwise, parameters such as permeability and fracture length can be seriously miscalculated.

In our study, we used the rate normalized pressure vs. material balance time, the normalized rate vs. square root of time, and the normalized rate vs. cumulative production plots, to obtain preliminary hydraulic fracture properties, reservoir permeability and original oil in place.

Geomechanics suggests that, in horizontal wells with multi-stage fractures, fracture often has symmetrical 'bi-wing' geometry. The model used in this workflow assumes that the fracture wings are two perfect rectangles, with a total length of x_{mf} as in Figure 35. For fully penetrating fractures the height of the rectangle is the formation thickness. To calculate the individual fracture length (x_f) for a well with n fractures we assume that $x_{mf}=n^* x_f$, as in the model proposed by Ambrose et al. (2011). See Figure 36.

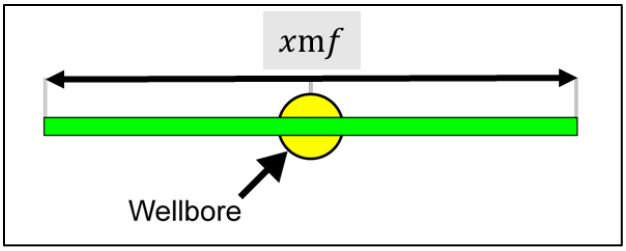

Figure 35 Single fracture intersecting the wellbore. This is the simplest model available in the Kappa software. (After KAPPA, 2003).

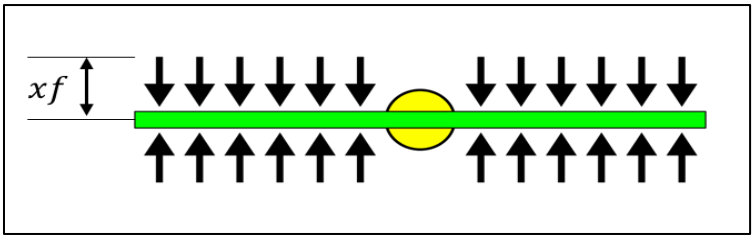

Figure 36 Equally spaced fractures, perpendicularly intersecting the well, each cluster generating a fracture. We assume that all fractures intersect the wellbore path at a 90° and that $x_{mf}=n^* x_f$. (After KAPPA, 2003).

The early time flow regime in a well with a high conductivity fracture is characterized on a log-log plot by a half slope on both the pressure and derivative curves.

The position of these two half slope straight lines will establish a link between the time and pressure match, providing a unique result for kx_{mf}^2. From the derivative we can calculate k, and the half fracture length will be calculated from kx_{mf}^2.

Figure 37 shows the log-log plot for well #1, with the help of the specialty lines (lines in Topaze NL that have a prefix ½ slope and 1 slope) and the values of t_{elf} , the end of the transient linear flow regime identified earlier in the workflow. The software created the linear flow half-slope line and the boundary dominated unit-slope line. The half-slope line provides us with the opportunity to estimate kx_{mf}^2. Since the permeability

range is known and since we can use the assumption that x_{mf} is the sum of all individual fracture half-lengths, i.e., $x_{mf}=n*x_f$, a first approximation for x_f was obtained. We used lateral length 3569ft for well 1, and we assumed that each of the 60 perforations (*cluster*perforations=12*5=60=n*) created a fracture, and we calculated x_f =239 ft. Table 2 summarizes the results from using the same methodology for wells #3 and well #4. Note that *n* can also be considered to be the number of fractures created.

If the permeability is unknown, the literature suggests many methods to estimate the permeability; however, in ultralow permeability reservoirs, the process will be an iterative, with convergence assumed when the analytical, empirical and numerical models match the data with the same value of permeability. Thus, we recommend that, even when the permeability value is known, we use all the tools available to ensure an appropriate fit of field data with the analytical model.

Using the square root of time plot, and fitting a straight line during the linear flow regime as shown in Figure 38, another value of x_f can be obtained following the logic mentioned earlier. Assuming that we create a fracture in each perforation, then we can estimate an independent value of. Table 3 shows that, following this methodology, x_f =241 ft is estimated for well 1.

While the two values of x_f found for every well are not exactly the same, they are similar in size and validate each other. These two graphical methodologies are important steps to establish a first approximation of fracture length to use in the analytical model.

The same procedure described for Well #1 was followed for Well #3 and Well #4, the values are in Table 2 and Table 3 and in Figure 40 to Figure 45 . The estimated

fracture lengths are similar to choose provided by the operator for wells #1 and #3. However, for well #4 our estimated fracture length is considerably smaller than the operator's, but the permeability near well 4 is larger, and we do not enough information to identify a single root cause of this discrepancy. It may be that the reservoir properties are different at the location of well 4, or perhaps there is a nearby well that affects fracture propagation.

Clarkson (2013) also pointed out that while obtaining an estimate of stock tank oil originally in place (STOIP) is not the main objective of most studies, the value of STOIP can be also acquired using the log-log and linear plots. Figure 39, known as the flowing material balance plot, can be used to calculate a rough estimate of STOIP using the boundary dominated flow regime data and extrapolating to a normalized rate of zero.

If a volumetric STOIP is calculated assuming the drainage volume of the well is simply the Stimulated Reservoir Volume– (SRV), another value of STOIP is acquired. However, this is an unrefined estimate. Table 4 summarizes the results for all 3 wells. Note that well length has a direct impact on STOIP; e.g., well #4 has larger STOIP than wells #1 and #3.

Table 1 Main Model Parameters results

Main Model Parameters				
	Well #1	**Well #3**	**Well #4**	**Units**
T_{min}	10	10	11.89	days
T_{max}	881	891	575	days
kh,	0.00254	0.00218	0.00621	md.ft
k, average	1.7E-5	1.45E-5	4.14E-5	md
Line: Slope 1 - closed system				
Area	34.9	35.6	50.6	acre
Circle radius	695	703	838	ft
Square size	1230	1250	1480	ft
Line: Slope 1/2 - fracture				
$k*x\mathrm{m}f^{2}$	3340	3150	9130	ft^2.md
$x\mathrm{m}f$	14030	14718	14848	ft

Table 2 Results from the Log-Log Plot

	Well #1	**Well #3**	**Well #4**	**Units**
k	1.70E-05	1.45E-05	4.14E-05	md
$k*x\mathrm{m}f^{2}$	3340	3150	9130	ft^2.md
$x\mathrm{m}f$	14030.8	14700	14848.27	ft
nf	12	14	19	
Fractures per Cluster	5	5	5	
xf	233.8	210.3	156.3	ft
Lw	3569	3897	6500	ft
conversion	5.614	5.614	5.614	bbl/ft^3

Table 3 Results from the square root of time plot

	Well #1	**Well #3**	**Well #4**	**Units**
k	1.70E-05	1.45E-05	4.14E-05	md
$kx_{\mathrm{m}f}{}^{2}$	3552	3329	13271	ft^2.md
$x_{\mathrm{m}f}$	14469.27	15130.67	17385	ft
nf	12	14	19	
Fractures per Cluster	5	5	5	
x_f	241.1546	216.1525	183	ft
L_w	3569	3897	6500	ft
conversion	5.614	5.614	5.614	bbl/ft^3

Table 4 Volumetrics STOIP using from model

	Well #1	Well #3	Well #4	Units
xf from Model	225	206	169	ft
h	150	150	150	ft
ϕ	0.07	0.07	0.07	ft^3/ft^3
S_w	0.3	0.3	0.3	
STOIP	1.401789	1.401365	1.917581	MMSTB

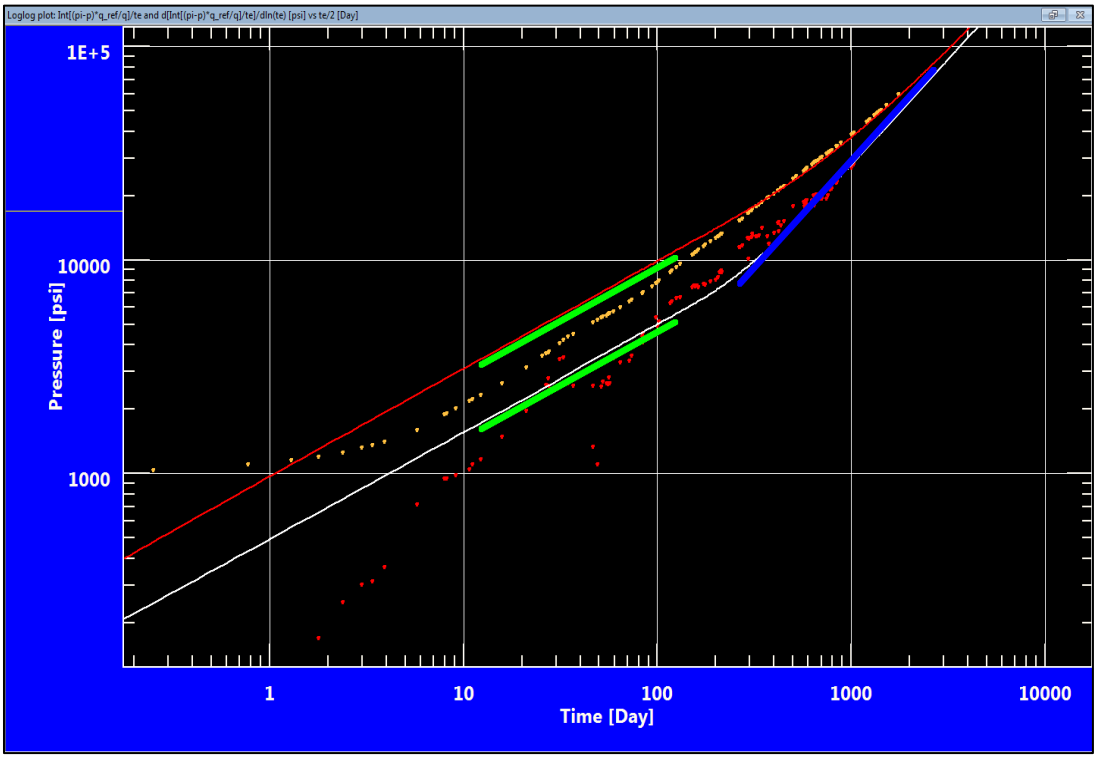

Figure 37 Well #1 log-log plot. Using MBT the linear flow regime was correctly placed and the boundary dominated period was also located. The transition region is clearer in this plot.

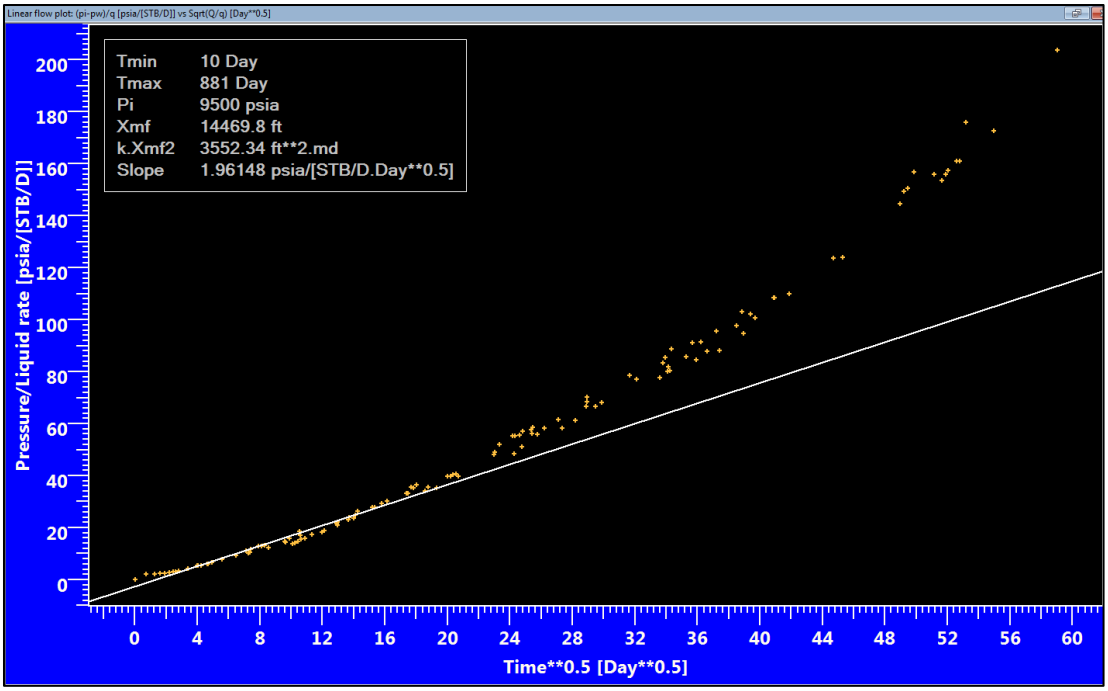

Figure 38 Well #1 square root of time plot. Even though a linear region can be found in several places, the MBT plot allowed us to apply linear regression to only the correct linear flow regime.

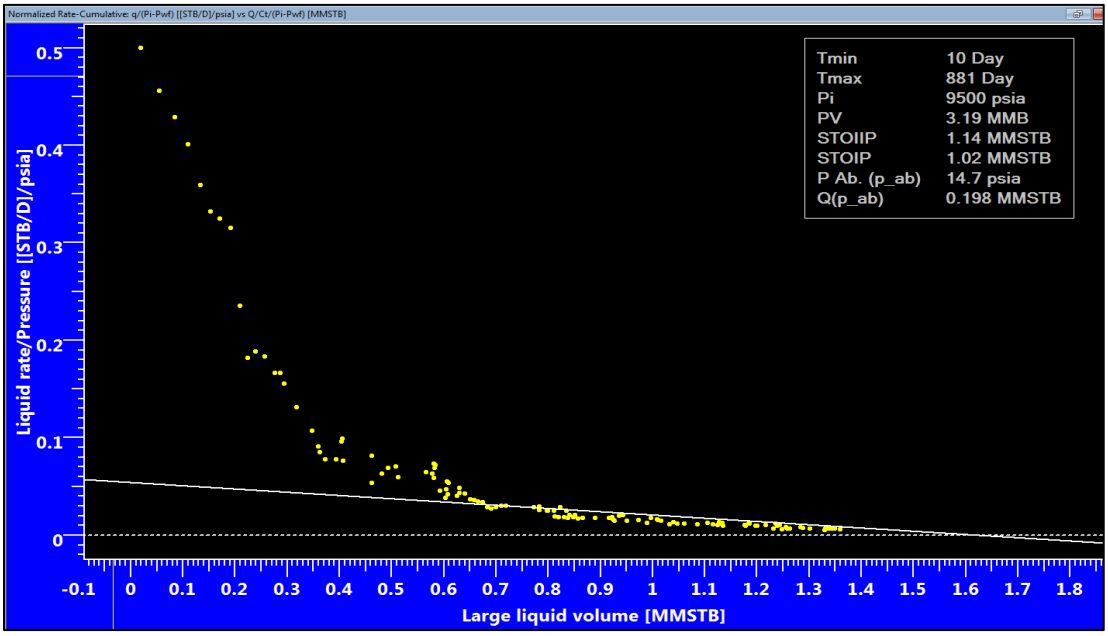

Figure 39 Well #1 normalized rate vs. cumulative production plot. The OOIP value in the plot is 1.14 MMSTB which differs by about 30% from the value found using the analytic al model.

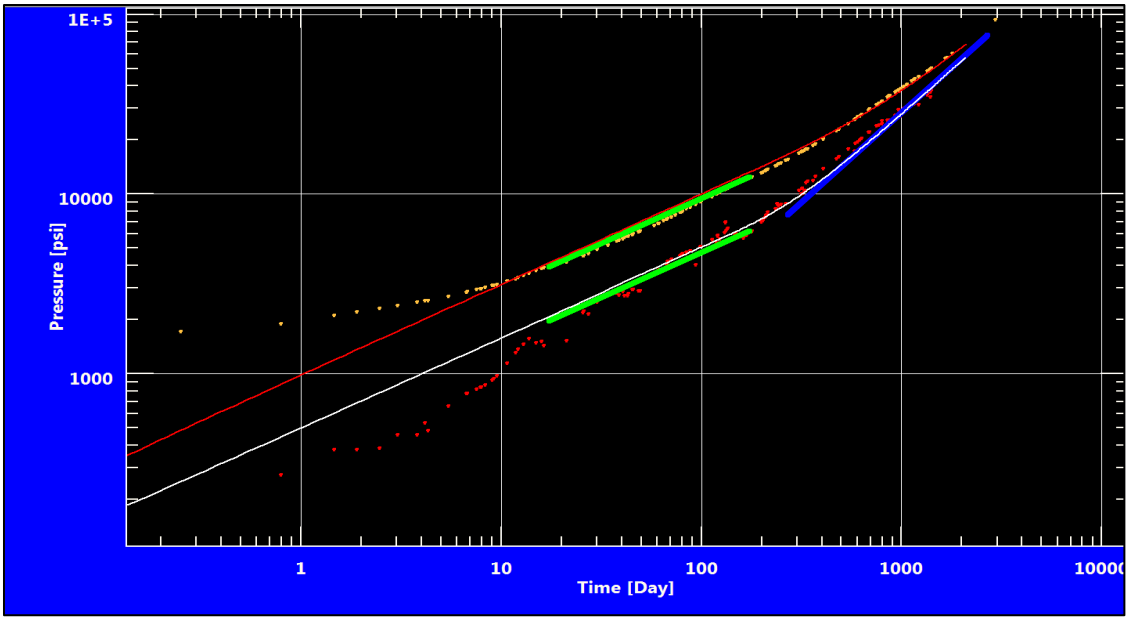

Figure 40 Well #3 log-log plot. The pressure derivative confirms the two flow regimes found with the MBT plot and it shows a short transition period. The derivative is quite noisy at early times.

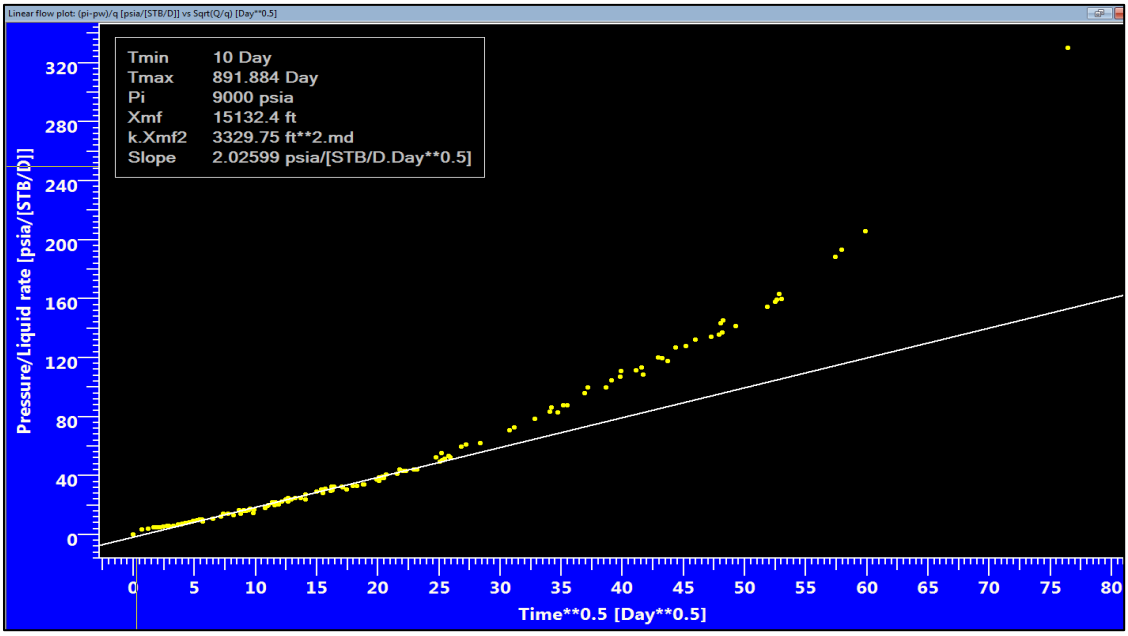

Figure 41 Well #3 square root of time plot. While a straight line could be fit in several places on the figure, the correct straight line is determined from the diagnostic plot.

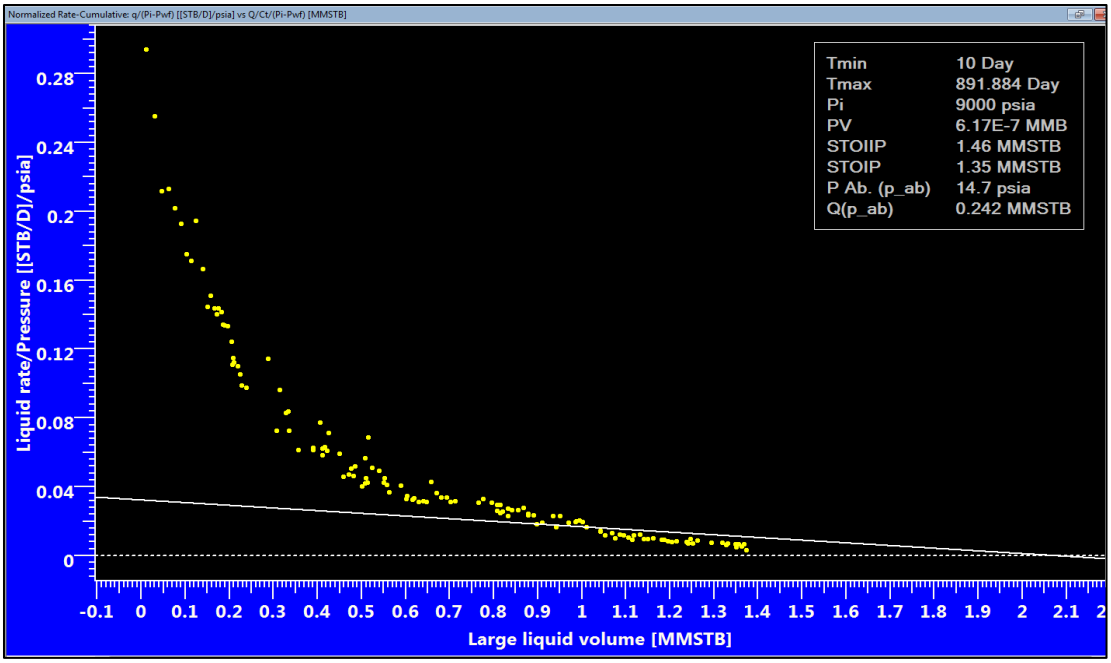

Figure 42 Well #3 Normalized rate vs. cumulative production plot. The regression line through the final data points is not clearly defined. Results from analysis of this plot are not as accurate as a volumetric calculation of STOIP.

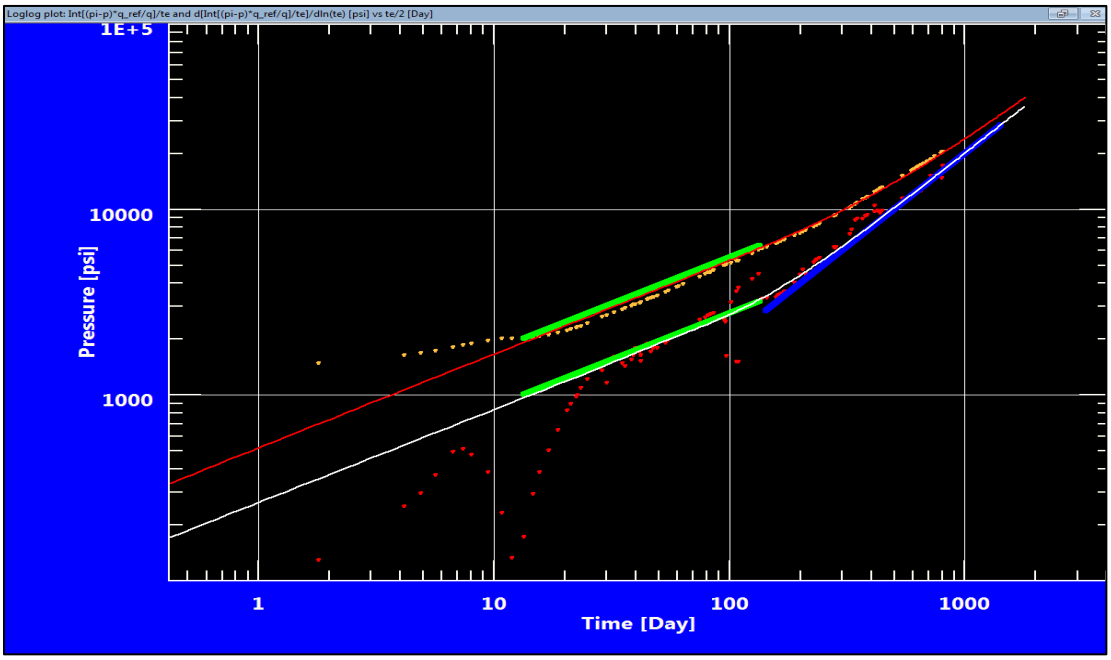

Figure 43 Well #4 log-log plot. Once the derivative stabilizes the half slope can be easily recognized and the boundary dominated flow regime is also apparent. The model matches the late time data well.

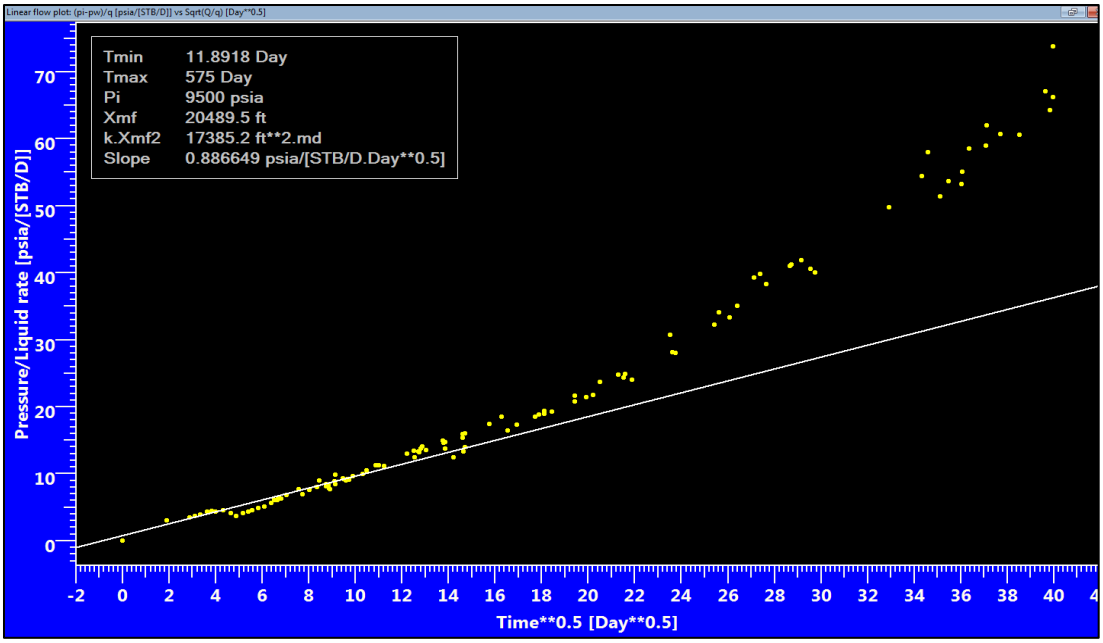

Figure 44 Well #4 square root of time plot. It is apparent that the linearity deteriorates beyond the end of the linear flow regime.

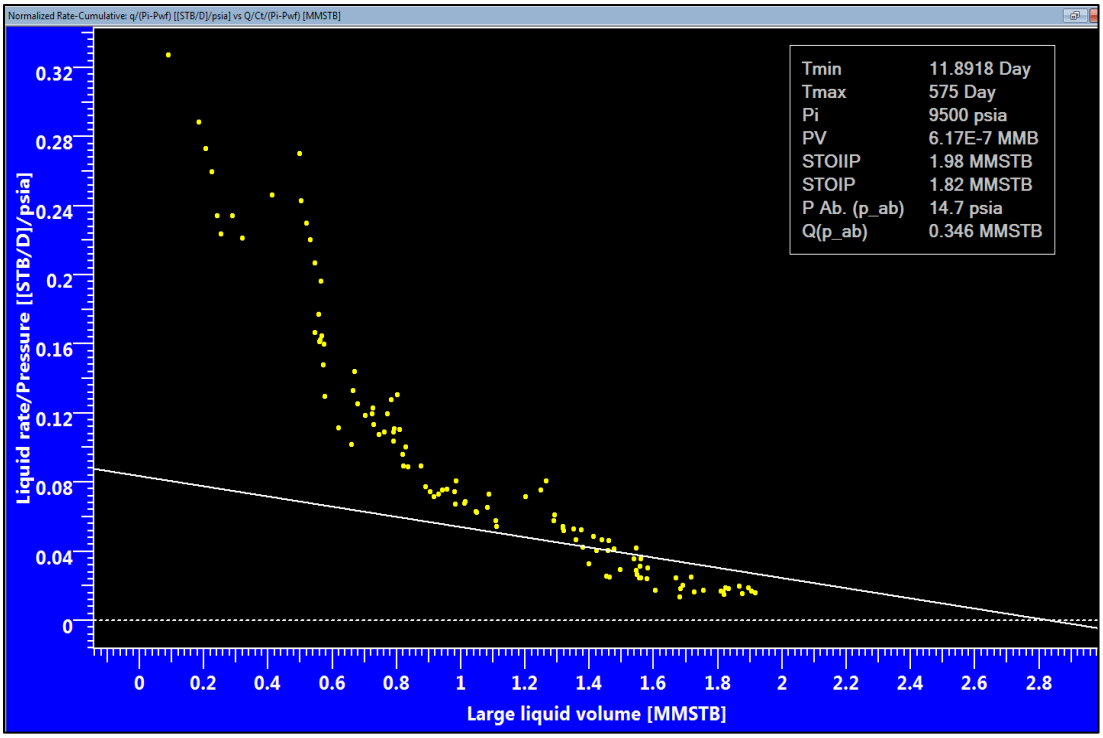

Figure 45 Well #4 Normalized rate – cumulative plot. This match is obviously not good, which can be explained by the relative lack of data at late times for this well.

STEP 6: FIND ANALYTICAL MODEL MATCH

For this step, Kappa Topaze NL was used. The software capabilities and features were described previously in step 5. With the reservoir properties estimated in step 5, a first run with an analytical model is possible. The initial estimates from step 5 are key components of the iterative history-matching step with analytical models. Once the parameters are acquired from the previous steps, iterations consistent with the physics of the reservoir are needed.

The importance of the analytical models in this workflow is that they can validate the fluid/rock behavior and interactions in the reservoir. History can be matched quickly and with many models at the same time. At this point, a major issue arises that Zhao et al. (2012) brought up with model matching in unconventionals: the non-uniqueness of the response.

This is where the importance of all the previous steps on the workflow come to light, because a model matched and with the wrong parameters and then used for forecasting will result in an invalid data set. A word of caution: the correct model might match only 80% of the field data, while an incorrect model may appear to match rates, cumulative oil and pressures even better.

Only when the model is deemed appropriate for the reservoir and the data can the forecast be recommended. Notice that forecasting with constant bottom hole pressure implies that the operational conditions will remain unchanged; this means that drilling wells nearby that interfere with drainage area, changing completions or alterations of the well architecture will deem the forecast invalid. There are several methods to terminate a

forecast: at the economic limit rate, at a physically minimum achievable rate or a combination of both. Terminal rate generally varies from company to company and even from internal reporting to external reporting.

Ozkan, et al. (2009) suggested that for MFHW the drainage volume be limited to the inner reservoir between the fractures even for relatively large matrix permeabilities. The authors suggested that the best model for low permeability reservoirs could be their trilinear-flow model.

The basis of Ozkan trilinear-flow model is the premise that the productive life of a multiply-fractured-horizontal-well is dominated by linear flow regimes shown in Figure 46. The trilinear-flow model couples linear flows in three contiguous flow regions: the outer reservoir, the inner reservoir between fractures, and in the hydraulic fracture.

This was the first model we used to fit to the data and to forecast production, but the forecast appeared to be extremely optimistic. When based only 1-2 years of production. The SRV bounded model (no flow from outside the SRV) was matched and considered to be a better fit of what is actually occurring in the reservoir.

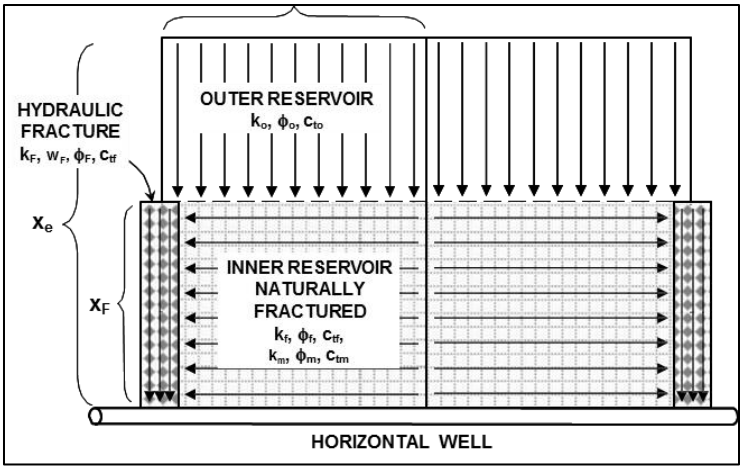

Figure 46 Schematic of the trilinear-flow model (after Okzan et al. 2009). The system is called trilinear because of the linear flow from the outer reservoir to the inner reservoir, the linear flow from the inner reservoir to the hydraulic fracture and the linear flow within the hydraulic fracture to the well.

Nobakht et al. (2012) proposed the SRV bounded model. In this model the reservoir is divided into two major parts, SRV and reservoir outside the SRV. The portion of reservoir directly influenced by the hydraulic fractures is known as SRV. Bello and Wattenbarger (2008) and Mayerhofer et al. (2006) reported that the contribution from the reservoir beyond the SRV is usually negligible in the case of extremely low permeability reservoirs; as a consequence, drainage beyond the SRV is insignificant. The SRV bounded model can be regarded as a special case of the trilinear flow model with negligible contribution from the outside reservoir. Alternatively, the trilinear model can be considered as a direct extension of the SRV bounded model with contribution from the outer zone modeled as a late time linear flow toward the fractured horizontal well.

For this particular set of wells, with the initial value of x_f ~250' and the permeability also known, we were ready to apply the input for the first pass of the numerical model. A first attempt was made to obtain a match between the models and the real data in all the relevant plots including the history plot. While this step may appear to

be unimportant, forced application of expertise and knowledge of the reservoir can be quite important.

The matches can start with the most basic model, which is the homogenous model for a vertical well with constant skin in a closed circle. This is obviously an inappropriate model but it could give the analyst a useful start in some cases. In this case, our initial assumed model was the trilinear model (Figure 47).

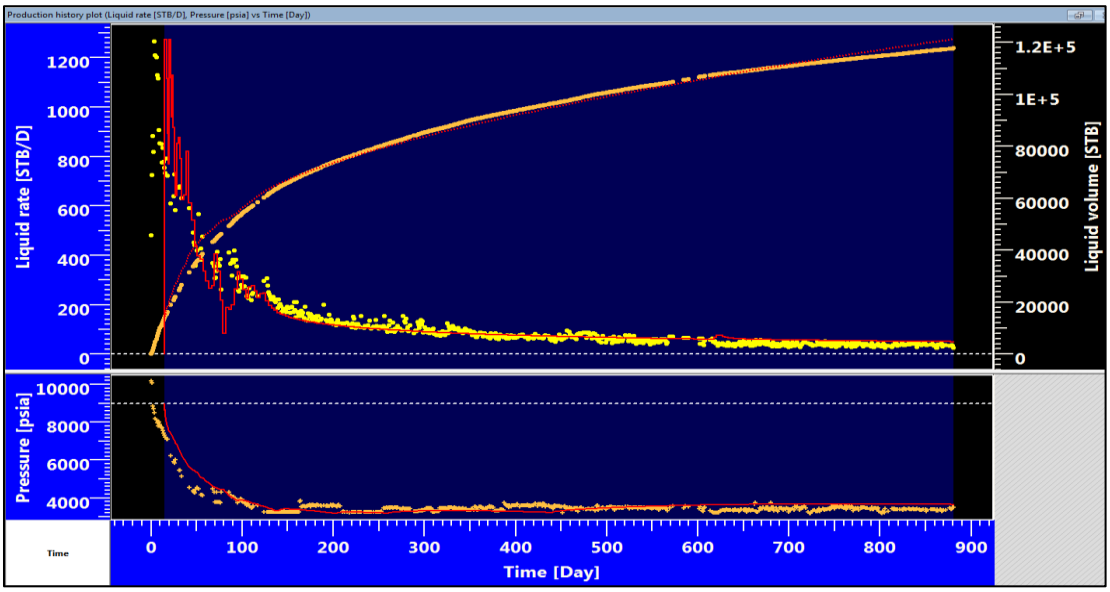

Figure 47 Trilinear model match for well #1. The figure shows how the trilinear model is a perfect match to the data set and how the early data is hard to be match due the data scattering.

An initial value of x_f ~250', obtained from the previous steps was used. As a second step in the model creation, we varied the x_f value to improve the fit to cumulative production, and to the rate in the late period. We did not attempt to improve the match of early data since the early data was noisy for all 3 wells in the study.

While the pressures, rates and cumulative production matches are excellent, when the model is used to generate forecasts it will assume that the outer matrix will continue

to drain into the well and historically this is likely in ultra-low permeability reservoirs. The issue with this assumption is not at the match itself; the more important consequences can be seen in the forecasts with such model, because they can be unrealistically optimistic.

Since this analysis is a sequential process, the SRV bounded model was selected as the next model that can match the data set. Once again the value of x_f was the main iteration parameter. This type of completion scenario assumes every hydraulic fracture connected to a perforated cluster is equal in length and height (Ambrose et al., 2011).

The infinite fracture conductivity model was also included on this model match and the assumption was that there is no pressure drop within the fractures. Figure 48 shows that this model has difficulties in matching match early data set but agrees well with late data.

The same procedure of model matching was followed for wells #3 and #4 (Figure 49 and Figure 50). The trilinear model with low matrix permeability the best match that we found for these the two wells; however, the SRV bounded model is the most accurate for the physics and mechanics of the reservoir. Table 5 summaries all the final values of match parameters for the three wells in the study.

While Topaze has an "improve" function that can be used with any parameter, this function can introduce even more variation in the model if values like initial pressure, number of fractures, wide ranges of permeability, effective well length or number of fractures start changing without reflecting the true reservoir characteristics.

This can create the perfect model match, but it will be a match that does not honor known reservoir and well values.

For all the wells in the data set, the improve function was used, since the value of x_f is very hard to estimate unless microseismic surveys are used regularly in the field or there is another means of establishing well interference. Also, the permeability was varied within the range of the values provided by the operator.

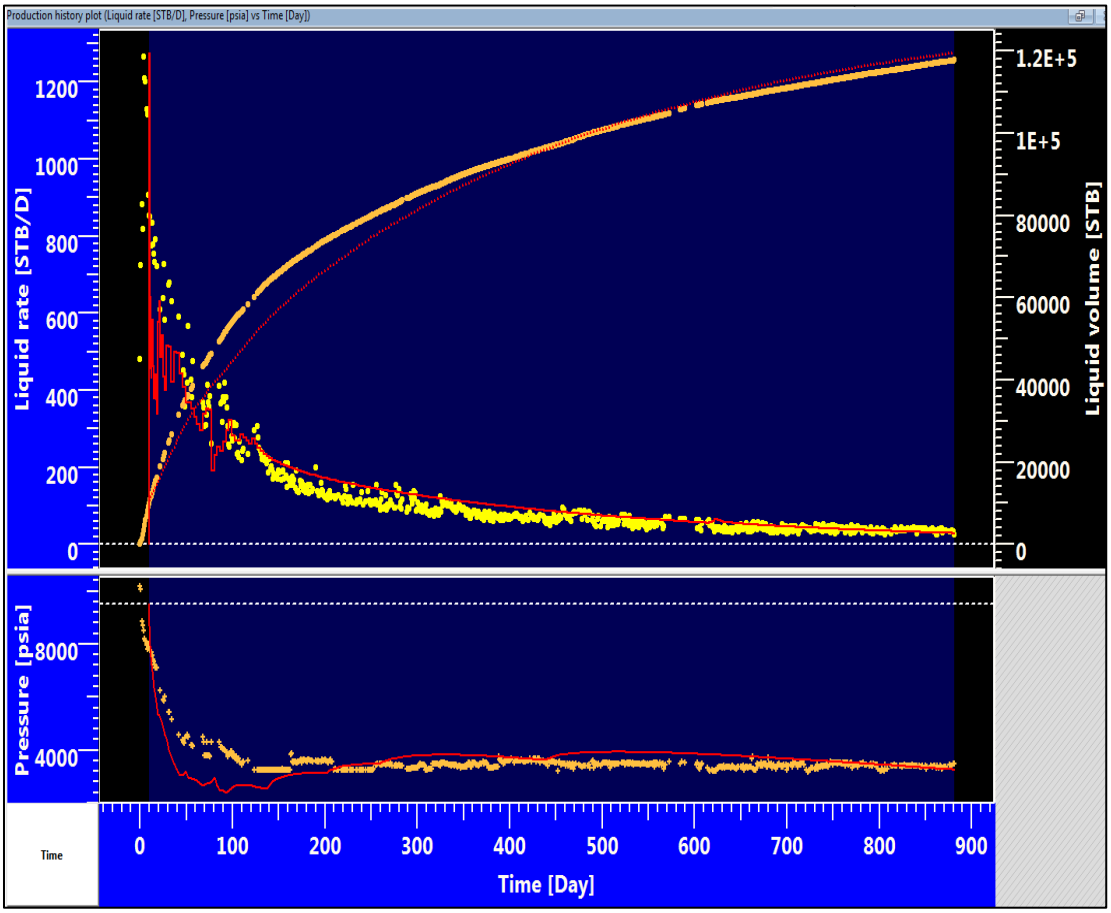

Figure 48 SRV bounded model match for Well #1. While the SRV bounded model does a poor job matching the early time of the data set, it does match the late time data, which is more important for forecasting.

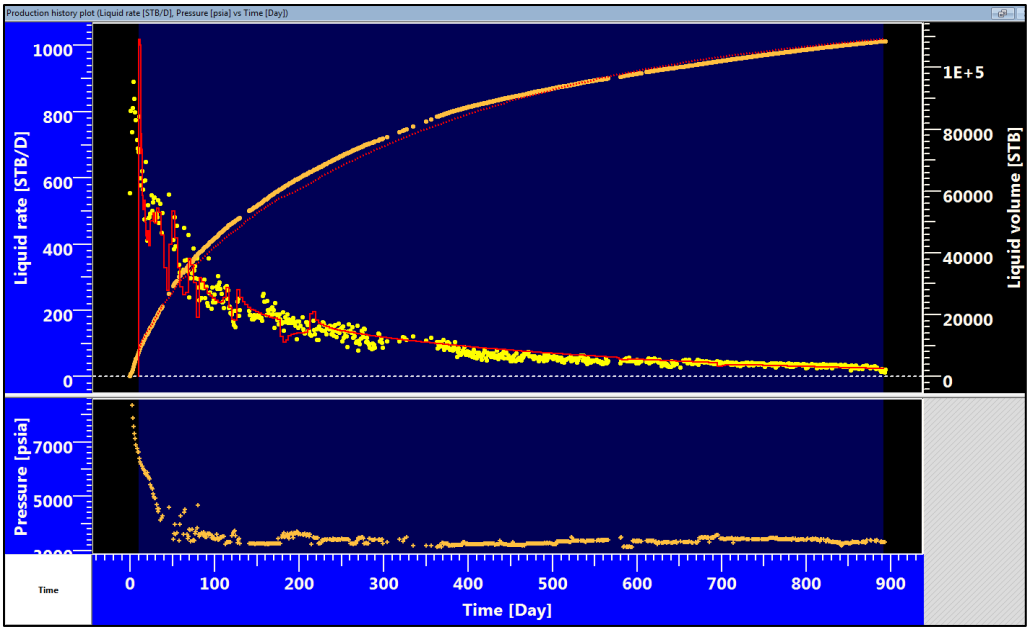

Figure 49 SRV model match for Well #3. It is quite apparent that the filter does a great job eliminating the outliers, however if the filter is applied strictly the early times will have little to no data left, affecting the model match even more.

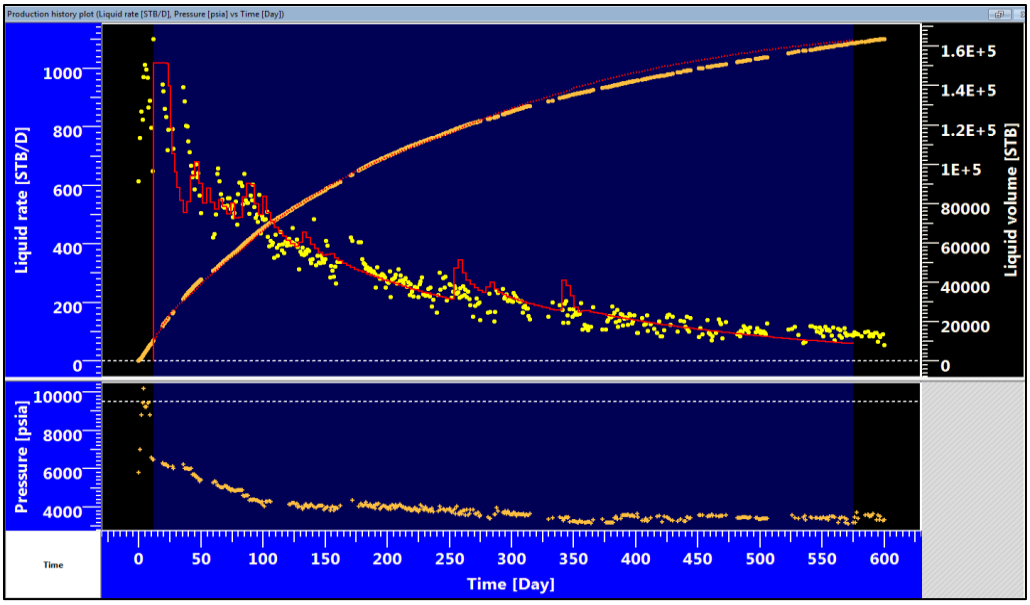

Figure 50 SRV model match for well #4. While there is a good correlation between pressure and rate, and the points that did not correlate were filtered out, the model is still sensitive to the pressure changes and tried to create an increased rates as pressure decreased. Late time changes in pressure were not accompanied by the expected decreases in rate; hence, we eliminated the points from the model match.

Table 5 SRV Model input and output for Well #1, Well#3 and Well #4

Model Option	**SRV Model Well 3**	**SRV Model Well 3**	**SRV Model Well #4**	
Main Model Parameters				
T_{min}	10	10	11.8918	Days
T_{max}	881	891.884	575	Days
k.h, total	0.00254	0.00218	0.00621	md.ft
k, average	1.7E-5	1.45E-5	4.14E-5	md
P_i	9500	9000	9500	psia
Reservoir & Boundary parameters				
h_w	3569	3897	6500	ft
Z_w	75	75	75	ft
Skin	0	0	0	--
No of Fractures	60	70	95	--
x_f of Fractures	225.371	206.376	169.857	ft
Fc of Fractures	5000	5000	5000	md.ft

STEP 7: TYPE CURVE ANALYSIS

Type curves in essence are preplotted solutions to flow equations, which are specific to different well/fracture geometries, reservoir types and boundary conditions. The objective of matching type curves to the data set on this workflow is to verify that the parameters found are in concordance with the ones found during the straight line analysis.

Extracted from Clarkson (2013) once the selection of type-curve set matching the identified model is done, it is followed by matching of the data to the type-curve and subsequently the extraction of hydraulic fracture/reservoir properties data from the type-curve match and ultimately the comparison of the derived properties with those obtained from straight-line analysis.

For MFHW in low permeability reservoirs, there have been recent developments in type curves generation, with the most popular among the current reservoir engineering community being the Bello and Wattenbarger (2010); this set of type curves is already included on the commercial version of Fekete Harmony (which is the KAPPA Topaze competitor) and it is currently use for volatile oil decline analysis plays like the Eagleford. The Fekete Harmony software was not available for this work.

For this particular data set the only type curves available in the kappa software were the Blasingame type curves. An attempt to match the data to the type curves was performed; as expected the match was not correct, because the only model available at the software is only suitable for multi-fractured vertical wells. These results can be seen on Table 6 and while the STOOIP is considerable underestimated the permeabilities values are within the expected range for the formation but the STOIP is within range of the one obtained on the previous steps.

Table 6 Blasingame Type curve plot results for Well #1, Well #3 and Well#4

	Well #1	Well #3	Well #4	
STOIP	1	1.17	1.53	MMSTB
R_e	692	748	855	ft
r_{wa}	0.39	0.244	0.192	ft
k	0.151	0.125	0.308	md
Skin	-0.531	-0.0638	0.179	--

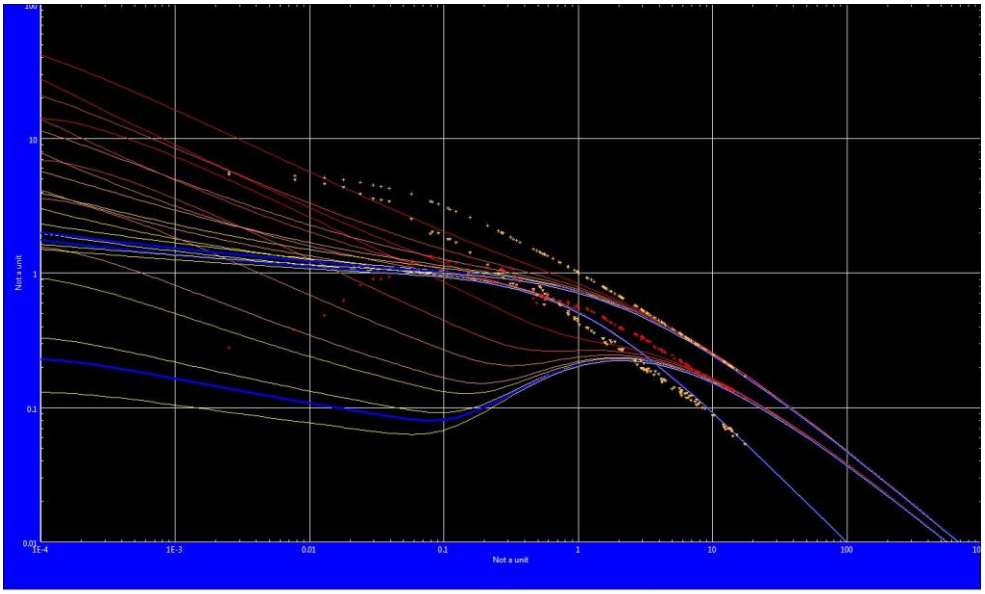

Figure 51 Well #1 Blasingame type curve match. It can be observed that the match is pretty poor as expected since the Blasingame model does not include MFHW.

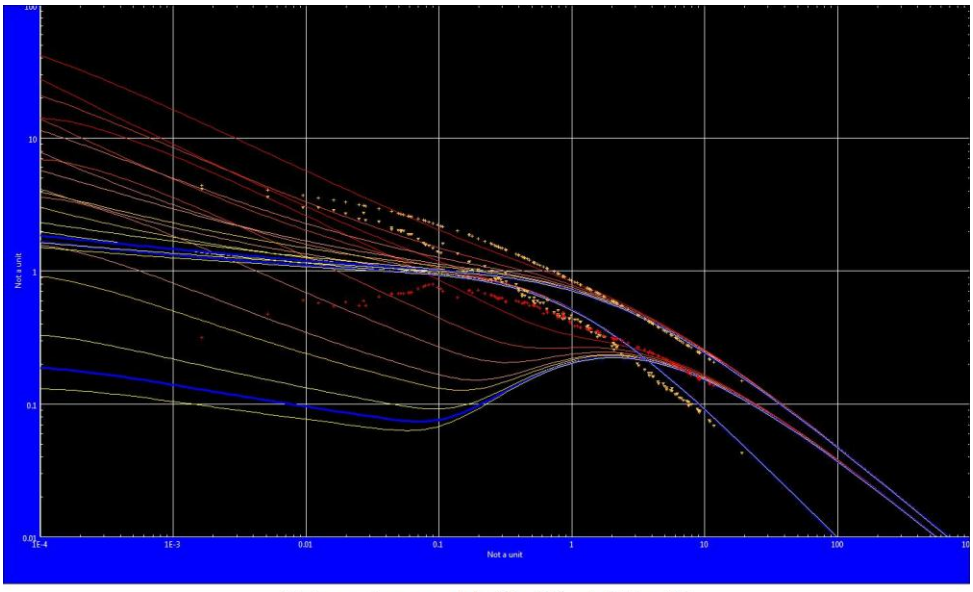

Figure 52 Well #3 Blasingame Type curve match. The match for this well is completely off, however this was an expected result due to the fact that this set of type curves are not designed for horizontal wells.

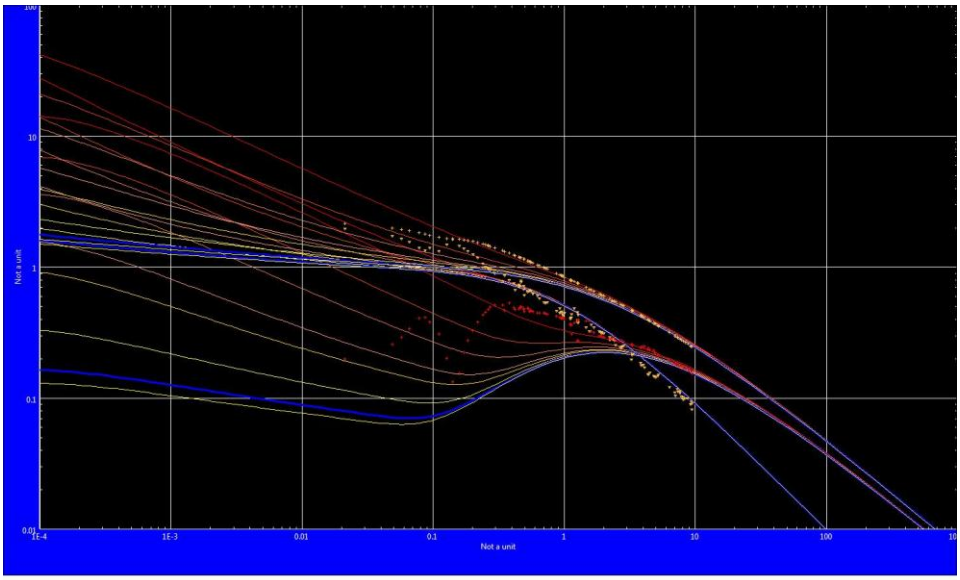

Figure 53 Well #4 Blasingame type curve match. The figure shows a very poor fit, if the type curves from Bello and Wattenbarger (2010) were the ones used, this fit might have been a better fit than the fit with Blasingame curves.

STEP 8: PERFORM FORECAST WITH ANALYTICAL MODEL

It cannot be stressed enough that a production forecasting analysis should be treated as a holistic process, even when the perfect match that is in agreement with all previous steps is found. After matching with an analytical model, we match with an appropriate empirical model. In this case, this the empirical model we used was a modified three-segment Arps model. The first segment is defined by the end of the linear flow; the second segment starts at the end of linear flow, until a need for a third segment is recognized visually. For this data set, this third segment was always added at the start of the forecast. This three-segment approach can be called a modified Arps model. A final quality check is not only extremely important, but also required. There are many possible fits based on empirical models; however, the analyst with all the knowledge acquired from the previous steps must ensure that not only a match with the analytical

model forecast is found, but that this particular match reflects the well/reservoir performance.

If more than one model fits the data well, once the match with the model is found, we recommend that the model be used to forecast and forecasted performance be examined to ensure that it is reasonable given what is expected under the current reservoir conditions. Our forecasts in this study assumed operating conditions will remain the same for the next 5 years. A longer period was selected first but the oil rate dropped below a reasonable economic limit in a short period of time, hence the 5 year well-life assumption. Operators can change future rates by changing operating conditions can select appropriate economic limit rates in a given situation.

Figure 54 shows the forecast using the SRV bounded reservoir model. The rate declines rapidly to values in the 1-2 BPD range three years into the forecast. The forecast is thus an excellent tool to predict when a workover might be performed to improve production. Figure 56 and Figure 57 show similar behavior for wells #3 and #4; suggesting that with the current completion in two years a re-stimulation to increase the size of the SRV may be in order to keep the wells producing.

Comparing the trilinear model and the SRV bounded model forecast for well #1 at Figure 54 and Figure 55, we see that, despite the trilinear model being a close fit for the data, it overestimates production at late times, not following the behavior observed in older wells in the area in which these wells are located. Such behavior was also predicted for wells #3 and #4.

The SRV bounded model was generated after finishing the workflow and trying to match the forecast with a multi-segment Arps model. This work highlighted the fact that the trilinear analytical model was not appropriate even though it provided a better overall match of the data, especially at early times.

This experience highlighted the fact that the workflow has to be done in sequential steps that ensure self-correction, meaning that the user cannot go blindly through the steps without comparing the results from the previous steps, checking for consistency and more importantly without taking into account the nature and observed behavior of the reservoir in study and the significance of an holistic approach to reserve estimations.

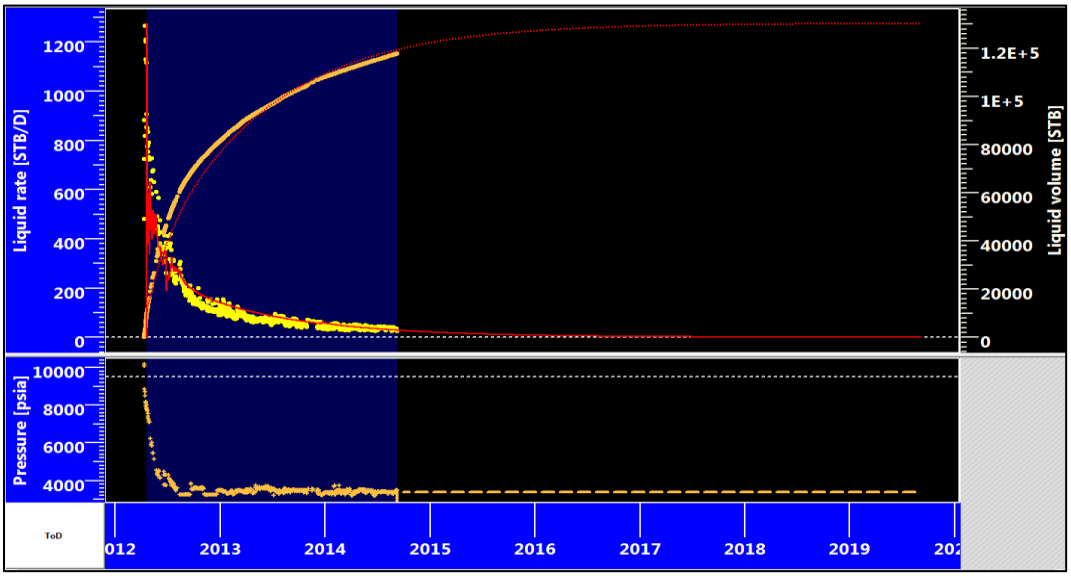

Figure 54 SRV bounded forecast for well #1. This forecast matches late time data well and assumes that the bottom hole pressure will remain constant until the end of the forecast.

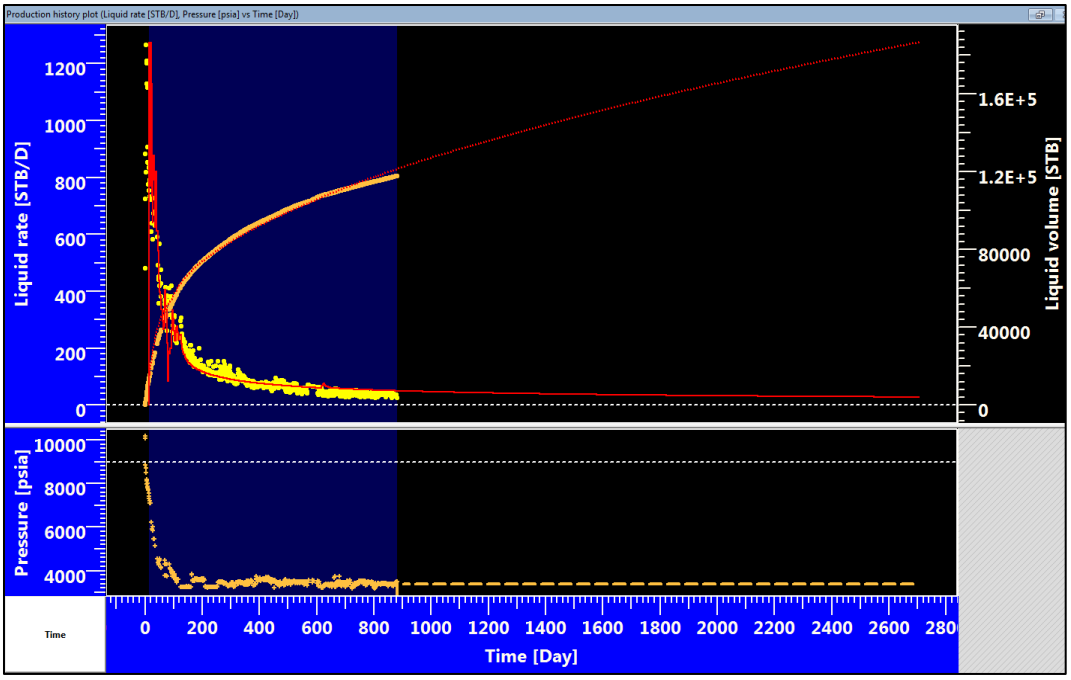

Figure 55 Trilinear model forecast for well #1. The forecast of future cumulative production is more optimistic than performance of other wells in the area suggests.

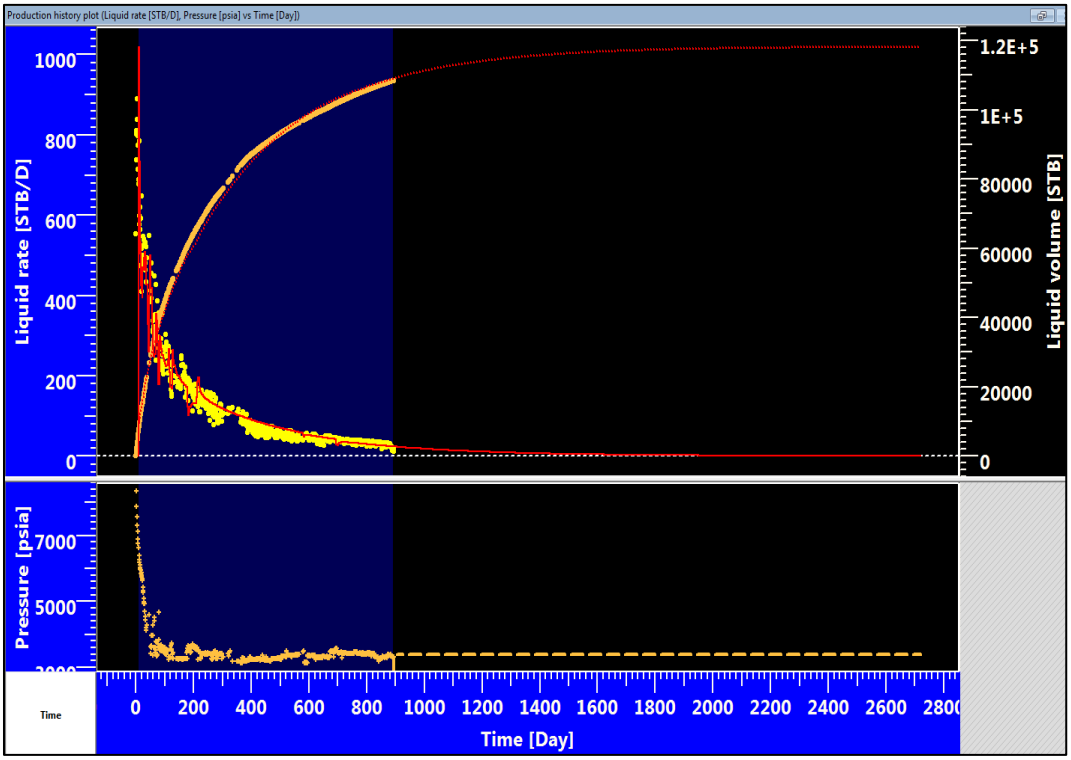

Figure 56 SRV Bounded model forecast for Well #3. This forecast better matches observed behavior in analog wells.

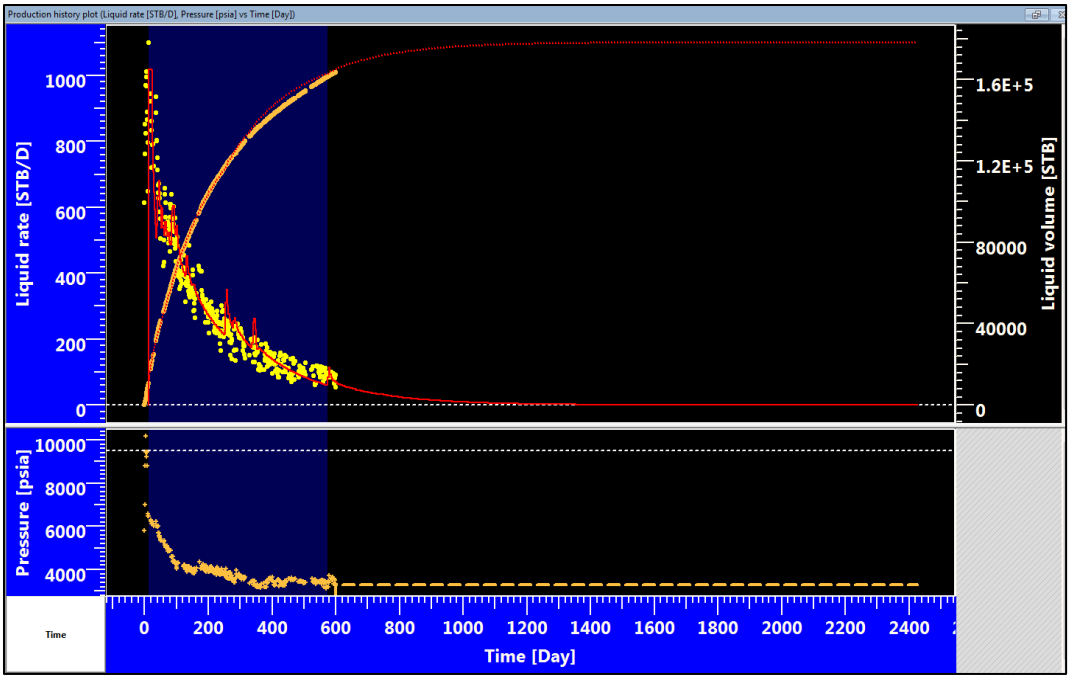

Figure 57 SRV bounded model forecast for Well #4. Despite the limited amount of production time for this well, the forecast matches the well behavior at later times.

STEP 9: FIT EMPIRICAL MODEL TO ANALYTICAL MODEL FORECAST

Oil and gas production rates decline naturally as a function of time. Loss of reservoir pressure or the changing relative volumes of the produced fluids are usually the cause. Fitting a curve through the performance history and assuming this same trend continues into the future forms the basis for decline curve analysis. The requirements for the correct application of Arps' decline models include the following: production at constant bottom hole pressure, boundary-dominated flow, fixed drainage area, unchanging radius of drainage with time, constant *b*, constant productivity index and unchanged skin factor.

It is well known that, in low and ultra-low permeability reservoirs, many of these conditions are not meet; since they remain in transient flow for long times, *b* is not constant and it decreases with time. Bottom-hole pressure also decreases with time. Thus, the Arps decline models are inappropriate in principle.

However many investigators, including us, have found ways to mitigate the problem. The first step is identify whether the wells are in transient flow or if they eventually reach boundary dominated flow, both of which occurred in the wells in this study. The next step is to determine whether the bottom hole pressure remains constant. This may be an artificially created situation due to a pump installation but it does impose the constraint. We can avoid the limitation of the requirement of production at constant BHP in most cases if we use normalized rate, $\frac{q}{(p_i - p_{wf})}$ instead of rate itself in our analysis. The third step is to assume that the drainage volume does not change with time, this is exactly what the premise of the SRV bounded model is once boundary-dominated flow is achieved. The fourth step is to address the changing *b* value; this is where using multiple *b* values assists us in applying the Arps model. In this workflow we recognized three distinct *b* values and three different D_i values.

Kupchenko et al. (2008) demonstrated that for a tight gas well in a bounded reservoir, the Arps *b* exponent changes from *b*=2 during the early linear flow and decreases during the transition to boundary-dominated flow. *b* then changed to 0.5 during boundary dominated flow. Kupchenko et al. went on to propose a *b* exponent fitting on transient data of *b*=2 and once boundaries are reached a *b*=<0.5 can be used based on the drawdown and the completion details.

The two segment model proposed by Nobakht et.al (2010) and Kupchenko et al. (2008) can be slightly modified and used to forecast production rates for this type of completion scenario. Topaze NL and Citrine software was used in this work to provide an analytical validation of the empirical forecasts.

There were three segments evident for all 3 wells: b=2 for the linear flow period with a D_i=0.1254 days^{-1}, a second segment starting from t_{elf} to the beginning of the forecast time with b=0.2 and D_i=0.003640 days^{-1} and a third segment from the forecast time until the end of the five years with b=0.2 and D_i=0.003943 days^{-1}. The behavior predicted with this approach is similar to that predicted by Nobakht et al. and Kupchenko et al. The EUR estimated with this match is 130.61 MSTB of oil and the analytical model forecast is 130.25 MSTB. The same procedure was applied to well #3and well #4 and the results can be seen on the Table 7 for all three wells in the data set and the match can be observed on the to Figure 58 to Figure 63.

While an acceptable match could have been achieved with a dual segment Arps model, a three segment model is recommended for a better match. However, if the accuracy of the results is secondary to speed, the dual segment Arps model, used by many, will be a more appropriate approach. The third segment can be based on a visual match, but in this study the third segment was based on final observed data and a smooth transition into the forecast.

The first segment was chosen with the help of the rate-MBT and the rate-time plots. Following the departure from linear flow, a second Arps segment with b=0.2 appears. The initial rate for this second segment is the final rate in the first segment, and D_i in the second segment is the final decline rate in the first segment. Time in the Arps

model for this period is elapsed time since the end of linear flow. The third initial rate is the final rate in the second segment, and the third D_i is the final decline rate in the second segment.

These three flow periods are observed consistently in all three wells. This corroborates the hypothesis that the wells are in similar reservoir rock and, if the completion procedures were the same, a forecast could be done for only one of the wells and applied to the others, if time were a limitation. Early data are not taken into account for the match; despite the data is being filtered, it is not on the same decline trend observed during the transient linear flow period; including it would introduce error in decline model parameters.

Initial rates also have significant impact on the match of the data and there could be many non-unique matches of the data, but honoring the data itself is preferred to the matching data without imposing constraints known from observations and knowledge of the reservoir.

Table 7 Analytical model forecast results for Well #1, Well #3 and Well #4

		Well #1	**Well #3**	**Well #4**
qi		1300 STBD	890 STBD	1200 STBD
Region 1	b	2	2	2
	D_i	0.1254 $days^{-1}$	0.052 $days^{-1}$	0.0208 $days^{-1}$
Region 2	b	0.2	0.2	0.2
	Di	0.003640 $days^{-1}$	0.003956 $days^{-1}$	0.005820 $days^{-1}$
Region 3	b	0.2	0.2	0.2
	Di	0.003943 $days^{-1}$	0.003582 $days^{-1}$	0.006766 $days^{-1}$
EUR @ 5 Years MSTB		130.61	118.45	179.18
TOPAZE Estimated Forecast MSTB		130.25	117.97	178.46

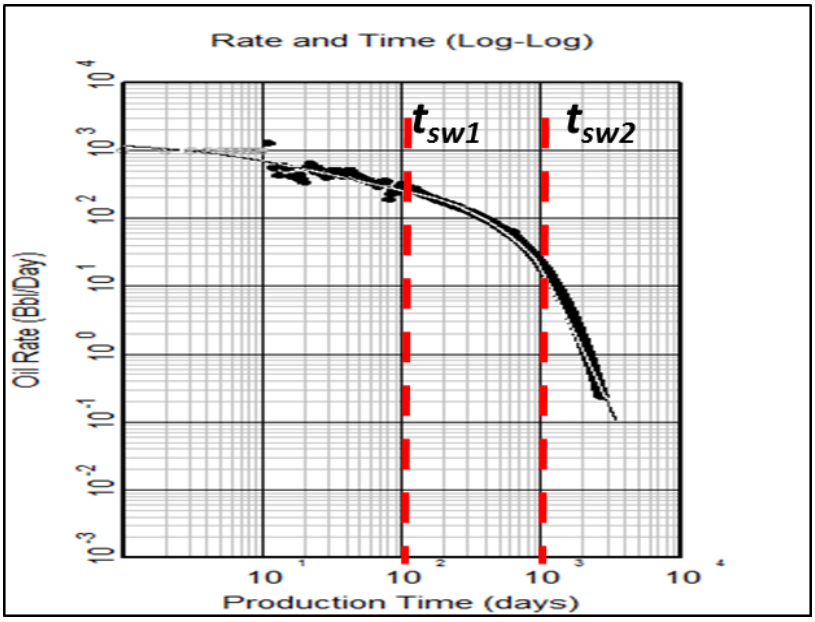

Figure 58 Rate and Time graph for Well #1. Two different switch times are indicated on the graph.

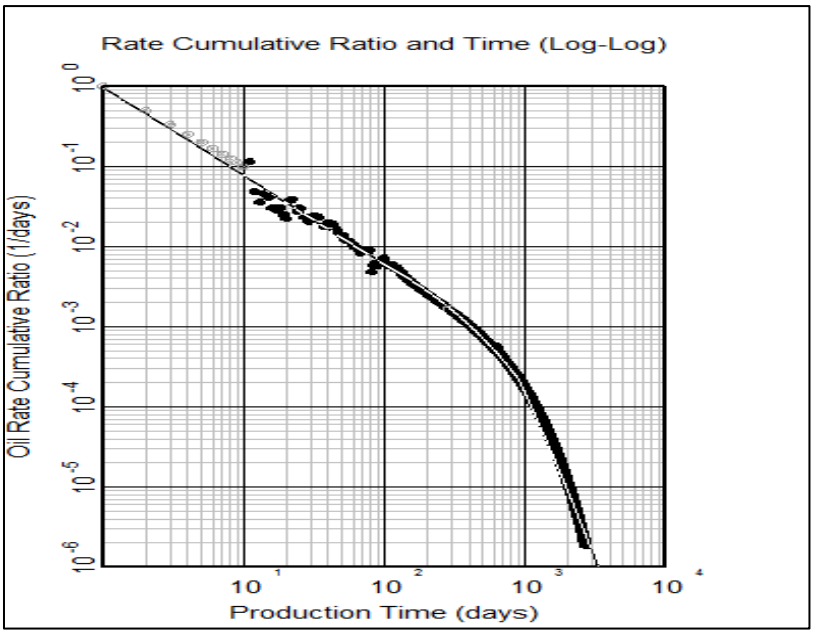

Figure 59 Rate cumulative ratio and time for well 1. The earlier data were not be matched, but the later data match is excellent and the match of the forecast from the analytical model is also excellent.

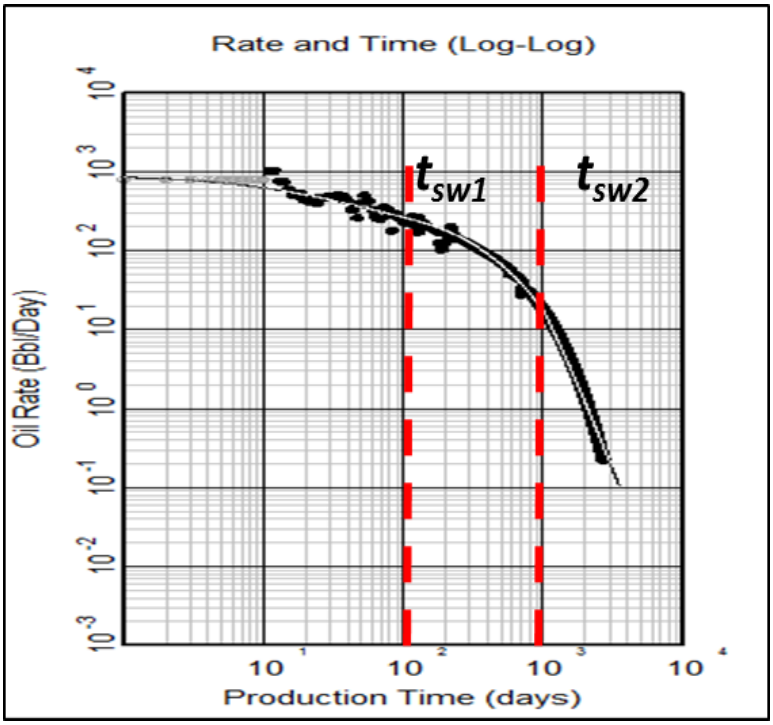

Figure 60 Rate vs. time graph for well #3. This figure shows the three different intervals where the proposed 3-segment Arps was applied, with good fits at all times.

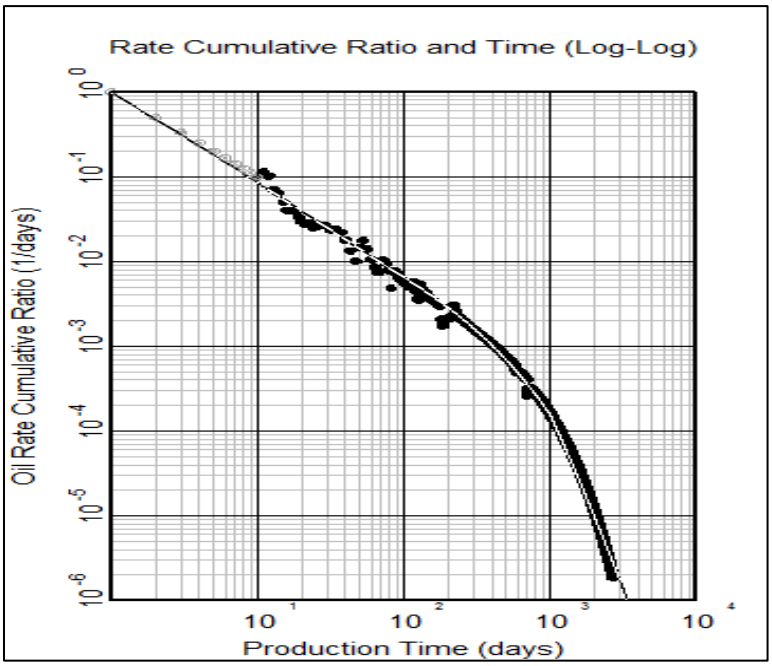

Figure 61 Rate cumulative ratio and time for well #3. The cumulative ratio scatters at earlier times but matches well at later times. The curvature of the line changes at exactly the same times we call the switch times.

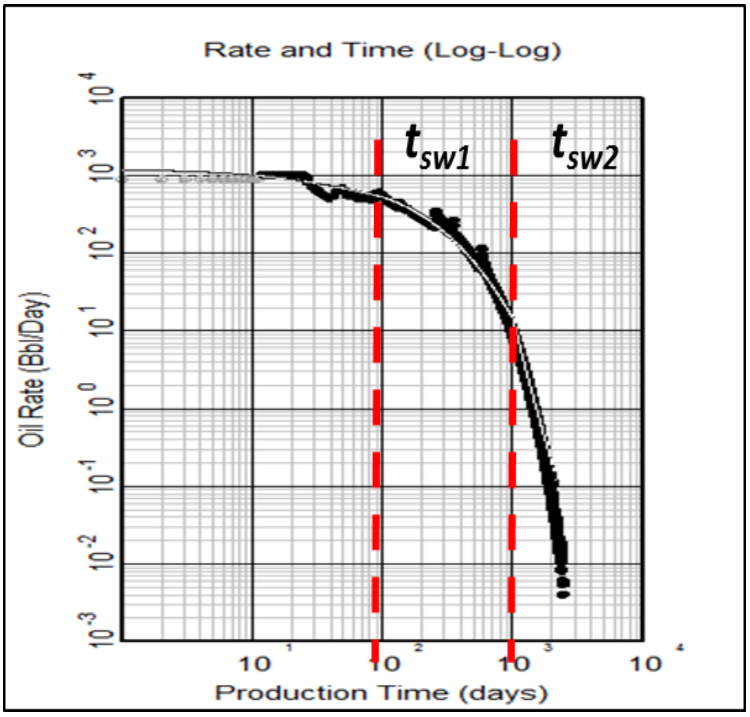

Figure 62 Rate and time graph for well #4. The early data are noisy, leading to matching difficulties.

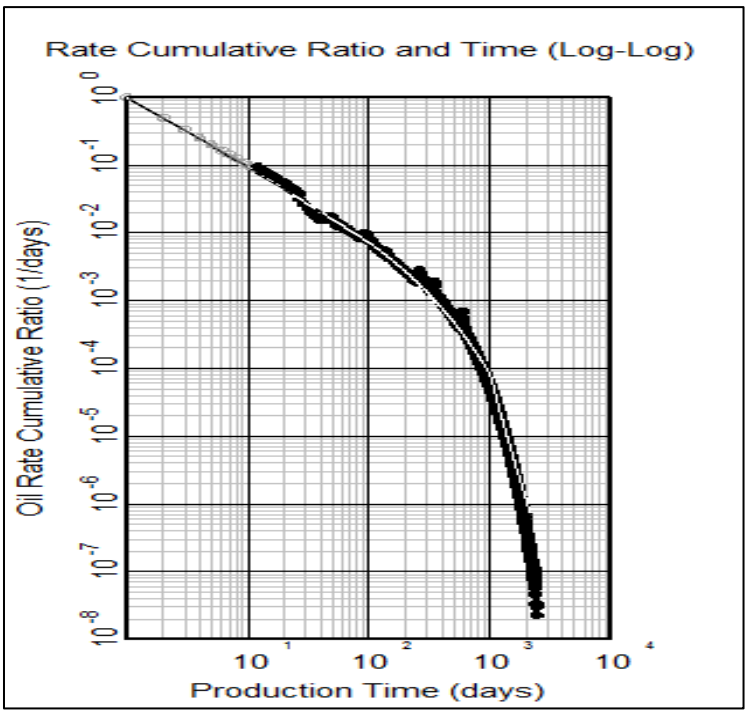

Figure 63 Rate cumulative ratio and time for well #4. Once again the dispersion of the data at early times make it matching difficult. A longer production history would help to refine the model.

CHAPTER 3 CONCLUSIONS

The workflow proposed by Clarkson (2013), initially developed to integrate the use of analytical and empirical production data analysis with the purpose of production forecasting/reserves estimations and reservoir characterization for gas reservoirs, was applied and validated for a volatile oil in this study. However, a limitation of this work is that the wells produced with single-phase flow in the reservoir, since pressure remained above bubble-point pressure. The decline trend could change after multiphase flow begins in the reservoir.

Data filtering using the Rastogi (2014) method helped to smooth the data; however, models were created with both raw and filtered data and the final outcome did not change significantly. The filter may be applied more appropriately to data sets with production histories longer than five years.

The seamless integration between the CITRINE and the TOPAZE workflows ensure the validation of an analytical reservoir model before forecasting production in order to base the forecast on sound science, avoiding the mere curve fitting usually associated with DCA.

The use of triple segment Arps for volatile oil production forecasting and reserve estimation is the most rapid forecasting method due to its simplicity and the fact that it respects the different flow regimes observed in the reservoir. A dual segment Arps can be used, however accuracy in forecasting may be compromised. And, of course, when multiphase flow begins in the reservoir, the decline trend may change.

REFERENCES

Al-Kobaisi, M., Ozkan, E., Kasogi, H., and Ramirez, B. 2006. Pressure-Transient Analysis of Horizontal Wells with Transverse, Finite-conductivity Fractures. Paper PETSOC 2006-126 presented at the Petroleum Society's 7th Canadian International Petroleum Conference (57th Annual Technical Meeting), Calgary, Alberta, Canada, 13-15 June, 2006. http://dx.doi.org/10.2118/2006-162

Ambrose, R. J., Clarkson C. R. , Youngblood, J. Adams, , Nyugen, P., Nobakht, M. and Biseda, B. 2011. Life-Cycle Decline Curve Estimation for Tight/Shale Gas Reservoirs. Paper SPE 140519 presented at the SPE Hydraulic Fracturing Technology Conference and Exhibition, The Woodlands, Texas, 24-26 January. http://dx.doi.org/10.2118/140519-MS

Arps. J. J. 1945. Analysis of Decline Curves. Transactions of AIME 168, 228-247. http://dx.doi.org/10.2118/945228-G

Bello, R.O., and Wattenbarger, R.A. 2008. Rate Transient Analysis in Naturally Fractured Shale Gas Reservoirs. Paper SPE 114591 presented at the CIPC/SPE Gas Technology Symposium 2008 Joint Conference, Calgary, Alberta, Canada, 16-19 June. http://dx.doi.org/10.2118/114591-MS

Chen, H.Y., Teufel, L.W. 2000. A New Rate-Time Type Curve for Analysis of Tight-Gas Linear and Radial Flows. Paper SPE 63094 presented at the SPE Annual Technical Conference and Exhibition, Dallas, Texas, USA, 1-4 October. http://dx.doi.org/10.2118/63094-MS

Clarkson, C.R., Jordan, C.L., Ilk, D., and Blasingame, T.A. 2009. Production Data Analysis of Fractured and Horizontal CBM Wells. Paper SPE 125929 presented at the 2009 SPE Eastern Regional Meeting, Charleston, West Virginia, USA, 23-25 September. http://dx.doi.org/10.2118/125929-MS

Clarkson, C. R., and Pedersen, P. K. 2010. Tight Oil Production Analysis: Adaptation of Existing Rate-Transient Analysis Techniques. SPE 137352 presented at the Canadian Unconventional Resources and International Petroleum Conference, 19-21 October, Calgary, Alberta, Canada. http://dx.doi.org/10.2118/137352-MS

Clarkson, C.R. 2013. Production data analysis of unconventional gas wells: Review of theory and best practices. International Journal of Coal Geology, Volumes 109-110, April 2013, Pages 101-146. http://dx.doi.org/10.1016/j.coal.2013.01.002

Houzé, O., Tauzin, E., Artus.V., Larsen, L. 2010. The Analysis Of Dynamic Data In Shale Gas Reservoirs- Part 1. KAPPA external publication.

Houzé, O., Viturat, D., Fjaere, S. 2003. Dynamic Data Analysis - v4.12.03. KAPPA external publications

Ilk, D., Valko, P., and Blasingame, T.A. 2007. A Deconvolution Method Based on Cumulative Production for Continuously Measured Flowrate and Pressure Data. Paper SPE 111269 presented at the 2007 SPE Eastern Regional Meeting, Lexington, Kentuky, USA, 17-19 October. http://dx.doi.org/10.2118/111269-MS

Ilk, D., Jenkins, C.D., and Blasingame, T.A. 2011. Production Analysis in Unconventional Reservoirs — Diagnostics, Challenges, and Methodologies. Paper SPE 144376 presented at the SPE North American Unconventional Gas Conference and

Exhibition, The Woodlands, Texas, USA, 14–16 June 2011. http://dx.doi.org/10.2118/144376-MS

Lee, W.J. 2013. SPEE Monograph 4, Chapter 4. Alternative Decline Models. SPE. On press.

Kupchenko, C. L. Gault, B. W. and Mattar, L. 2008. Tight Gas Production Performance using Decline Curves. Paper SPE 114991 presented at the CIPC/SPE Gas Technology Symposium, Calgary, Alberta, Canada, 16-19 June. http://dx.doi.org/10.2118/114991-MS

Mayerhofer, M.J., Stutz, H.L., Davis, E.J., Wolhart, S.L. 2006. Optimizing Fracture Stimulation Using Treatment-Well Tiltmeters and Integrated Fracture Modeling. Paper SPE 84490 presented at the 2003 SPE Annual Technical Conference and Exhibition, Denver, Colorado, USA, 5-8 October. http://dx.doi.org/10.2118/84490-PA

Nobakht, M., Ambrose R. and Clarkson, C.R. 2011. Effect of Heterogeneity in a Horizontal Well with Multiple Fractures on the Long-Term Forecast in Shale Gas Reservoirs. Paper CSUG/SPE 149400 presented at the Canadian Unconventional Resources Conference, Calgary, Alberta, Canada, 15-17 November. http://dx.doi.org/10.2118/149400-MS

Nobakht, M, Clarkson, C.R. 2012. Hybrid Forecasting Methods for Multi-Fractured Horizontal Wells: EUR Sensitivities. Paper SPE 153220 presented at the SPE Middle East Unconventional Gas Conference and Exhibition, Abu Dhabi, UAE, 23-25 January. http://dx.doi.org/10.2118/153220-MS

Palacio, J.C., Blasasingame, T.A. 1993. Decline-Curve Analysis With Type Curves – Analysis of Gas Well Production Data. Paper SPE 25909 presented at the SPE Rocky

Mountain Regional/Low Permeability Reservoirs Symposium, Denver, Colorado, USA, 12-14 April. http://dx.doi.org/10.2118/25909-MS

Rastogi, A. 2014. Production Forecasting Using Type Wells, Diagnostic Plots and Hybrid Models. Master's Thesis, University of Houston, Houston, Texas, USA

Song, B. and Ehlig-Economides, C. 2011. Rate-Normalized Pressure Analysis for Determination of Shale Gas Well Performance. Paper SPE 144031 presented at the SPE North American Unconventional Gas Conference and Exhibition, The Woodlands, Texas, USA, 14-16 June. http://dx.doi.org/10.2118/144031-MS

Valko, P.P. 2009. Assigning Value to Stimulation in the Barnett Shale: A Simultaneous Analysis of 7000 Plus Production Histories and Well Completion Records. Paper SPE 119369 presented at the SPE Hydraulic Fracturing Technology Conference, The Woodlands, Texas, 19-21 January. http://dx.doi.org/10.2118/119369-MS.

Yu, S. and Miocevic, D. J. 2013. An Improved Method to Obtain Reliable Production and EUR Prediction for Wells with Short Production History in Tight/Shale Reservoirs. Paper SPE 168684 presented at the SPE Unconventional Resources Technology Conference, Denver, Colorado, USA, 12-14 August. http://dx.doi.org/10.1190/URTEC2013-003

Zhao, V., Gupta, S., Banerjee, R., Poe, B., Spath, J. and Thambynayagam, M. 2013. Production Forecasting and Analysis for Unconventional Resources. Paper IPTC 17176 presented at the International Petroleum Technology Conference, Beijing, China, 26-28 March. http://dx.doi.org/10.2118/155737-MS